

Pathwise Conditioning of Gaussian Processes

James T. Wilson*

Imperial College London

J.WILSON17@IMPERIAL.AC.UK

Viacheslav Borovitskiy*

St. Petersburg State University and

St. Petersburg Department of Steklov Mathematical Institute of Russian Academy of Sciences

VIACHESLAV.BOROVITSKIY@GMAIL.COM

Alexander Terenin*

Imperial College London

A.TERENIN17@IMPERIAL.AC.UK

Peter Mostowsky*

St. Petersburg State University

PMOSTOWSKY@GMAIL.COM

Marc Peter Deisenroth

University College London

M.DEISENROTH@UCL.AC.UK

Abstract

As Gaussian processes are integrated into increasingly complex problem settings, analytic solutions to quantities of interest become scarcer and scarcer. Monte Carlo methods act as a convenient bridge for connecting intractable mathematical expressions with actionable estimates via sampling. Conventional approaches for simulating Gaussian process posteriors view samples as vectors drawn from marginal distributions over process values at a finite number of input location. This distribution-based characterization leads to generative strategies that scale cubically in the size of the desired random vector. These methods are, therefore, prohibitively expensive in cases where high-dimensional vectors—let alone continuous functions—are required. In this work, we investigate a different line of reasoning. Rather than focusing on distributions, we articulate Gaussian conditionals at the level of random variables. We show how this *pathwise* interpretation of conditioning gives rise to a general family of approximations that lend themselves to fast sampling from Gaussian process posteriors. We analyze these methods, along with the approximation errors they introduce, from first principles. We then complement this theory, by exploring the practical ramifications of pathwise conditioning in a various applied settings.

Keywords: Gaussian processes, approximate posteriors, efficient sampling.

1. Introduction

In machine learning, the narrative of Gaussian processes is dominated by talk of distributions (Rasmussen and Williams, 2006). Given the backdrop of Bayesian methods for regression and classification, compelling arguments exist to explain for the continued success and popularity of this vantage point. Rather than inferring an actual function that explains for the data, thinking about stochastic processes in terms of their marginal distributions allows us to focus on its behavior at a finite set of training and test locations. Because we may trivially marginalize out subsets of jointly Gaussian random variables, this shift in

*Equal contribution.

focus—from functions to marginal distributions—not only simplifies discourse but facilitates practical implementation.

In the real world, model-based inference and prediction typically service some broader goal. For example, when making decisions in the face of uncertainty, models play a crucial role by enabling us to simulate the consequences of our actions. Decision-making then amounts to optimizing the expectation of a simulated quantity of interest, such as a reward. Be it for purposes of safety or for balancing trade-offs between short-term and long-term rewards, it is crucial that these simulations faithfully portray both knowledge and uncertainty. Gaussian processes make accurate, well-calibrated predictions and, therefore, stand as the model-of-choice in fields, such as Bayesian optimization (Shahriari et al., 2015), uncertainty quantification (Bect et al., 2012), and model-based reinforcement learning (Deisenroth and Rasmussen, 2011).

Simulations and distributions do not always go hand in hand, however. While quantities defined in terms of process values at individual locations \mathbf{x}_* can be readily evaluated based on marginal distributions, the same cannot be said of quantities defined over collections of locations \mathbf{X}_* . Standard distribution-based strategies for sampling from GP posteriors scale prohibitively with the number of test locations \mathbf{X}_* . In these cases then, we may be better off thinking about GP from a different perspective.

In the early 1970s, one such view surfaced in the then nascent field of geostatistics (Journel and Huijbregts, 1978; Chiles and Delfiner, 2009). Rather than focusing on the statistical properties of Gaussian random variables, “conditioning by Kriging” encourages us to think in terms of the variables themselves. We study the broader implications of this paradigm shift to develop a general framework for conditioning Gaussian processes at the level of random functions. Formulating conditioning in terms of sample paths, rather than distributions, allows us to separate out the effect of the prior from that of the data. By leveraging this property, *pathwise conditioning* enables us to efficiently approximate actual function draws from GP posteriors. Along with a host of additional benefits, this reduces the cost of sampling process values $\mathbf{f}_* = f(\mathbf{X}_*)$ from $\mathcal{O}(*^3)$ to $\mathcal{O}(*)$.

The general structure of the remaining text is as follows. Section 2 and Section 3 explore pathwise conditioning of multivariate normal vectors and Gaussian processes, respectively. Section 4 surveys strategies for approximating function draws from GP priors, and Section 5 discusses different means of constructing update functions that combine with draws from the prior to represent the posterior. Section 6 studies the behavior of errors introduced by different approximation techniques, while Section 7 complements this theory with a bit of empiricism. Section 8 concludes.

Notation By way of example, we denote matrices as \mathbf{A} and (random) vectors as \mathbf{a} . We write $\mathbf{x} = \mathbf{a} \oplus \mathbf{b}$ for the direct sum of vectors \mathbf{a} and \mathbf{b} . When dealing with a covariance matrix $\Sigma = \text{Cov}(\mathbf{x}, \mathbf{x})$, we use subscripts to identify corresponding blocks, i.e., $\Sigma_{\mathbf{a}, \mathbf{b}} = \text{Cov}(\mathbf{a}, \mathbf{b})$. As shorthand, we denote the evaluation of a (random) function $f : \mathcal{X} \rightarrow \mathbb{R}$ at a finite set of locations $\mathbf{X}_* \subseteq \mathcal{X}$ by the (random) vector \mathbf{f}_* . Putting these together, when dealing with random variables $\mathbf{f}_* = f(\mathbf{X}_*)$ and $\mathbf{f}_n = f(\mathbf{X}_n)$, we write $\mathbf{K}_{*,n} = \text{Cov}(\mathbf{f}_*, \mathbf{f}_n)$.

2. Conditioning Gaussian distributions and random variables

A random vector $\mathbf{x} = (x_1, \dots, x_n) \in \mathbb{R}^n$ is said to be Gaussian if there exists a matrix \mathbf{L} and vector $\boldsymbol{\mu}$ such that

$$\mathbf{x} \stackrel{d}{=} \boldsymbol{\mu} + \mathbf{L}\boldsymbol{\zeta} \quad \boldsymbol{\zeta} \sim \mathcal{N}(\mathbf{0}, \mathbf{I}), \quad (1)$$

where $\mathcal{N}(\mathbf{0}, \mathbf{I})$ is known as the standard version of a (multivariate) normal distribution, which is defined through its density. Each such distribution is uniquely identified by its first two moments: its mean $\boldsymbol{\mu} = \mathbb{E}(\mathbf{x})$ and its covariance $\boldsymbol{\Sigma} = \mathbb{E}[(\mathbf{x} - \boldsymbol{\mu})(\mathbf{x} - \boldsymbol{\mu})^\top]$. Its corresponding probability density function is then defined as

$$p(\mathbf{x}) = \mathcal{N}(\mathbf{x}; \boldsymbol{\mu}, \boldsymbol{\Sigma}) = \frac{1}{\sqrt{|2\pi\boldsymbol{\Sigma}|}} \exp\left(-\frac{1}{2}(\mathbf{x} - \boldsymbol{\mu})^\top \boldsymbol{\Sigma}^{-1}(\mathbf{x} - \boldsymbol{\mu})\right). \quad (2)$$

The representation of \mathbf{x} given by (1) is commonly referred to as its *location-scale* form and stands as the most widely used method for sampling Gaussian random vectors. Since $\boldsymbol{\zeta}$ has identity covariance, any matrix square root of $\boldsymbol{\Sigma}$, such as the Cholesky factor \mathbf{L} with $\boldsymbol{\Sigma} = \mathbf{L}\mathbf{L}^\top$, may be used to draw \mathbf{x} as prescribed by (1).

Here, we focus on multivariate cases $n > 1$ and investigate different ways of reasoning about conditional random variables $\mathbf{a} \mid \mathbf{b} = \boldsymbol{\beta}$ for non-trivial partitions $\mathbf{x} = \mathbf{a} \oplus \mathbf{b}$.

2.1 Distributional conditioning

The quintessential approach to deriving the distribution of \mathbf{a} subject to the condition $\mathbf{b} = \boldsymbol{\beta}$ taught in elementary statistics courses employs the usual set of matrix identities to factor $p(\mathbf{b})$ from $p(\mathbf{a}, \mathbf{b})$. Applying Bayes' rule, $p(\mathbf{b})$ then cancels out and $p(\mathbf{a} \mid \mathbf{b} = \boldsymbol{\beta})$ is identified as the remaining term—namely, the Gaussian distribution $\mathcal{N}(\boldsymbol{\mu}_{\mathbf{a}|\boldsymbol{\beta}}, \boldsymbol{\Sigma}_{\mathbf{a},\mathbf{a}|\boldsymbol{\beta}})$ with moments

$$\boldsymbol{\mu}_{\mathbf{a}|\boldsymbol{\beta}} = \boldsymbol{\mu}_{\mathbf{a}} + \boldsymbol{\Sigma}_{\mathbf{a},\mathbf{b}}\boldsymbol{\Sigma}_{\mathbf{b},\mathbf{b}}^{-1}(\boldsymbol{\beta} - \boldsymbol{\mu}_{\mathbf{b}}) \quad \boldsymbol{\Sigma}_{\mathbf{a},\mathbf{a}|\boldsymbol{\beta}} = \boldsymbol{\Sigma}_{\mathbf{a},\mathbf{a}} - \boldsymbol{\Sigma}_{\mathbf{a},\mathbf{b}}\boldsymbol{\Sigma}_{\mathbf{b},\mathbf{b}}^{-1}\boldsymbol{\Sigma}_{\mathbf{b},\mathbf{a}}. \quad (3)$$

Following the previous section then, the conventional way of obtaining samples from $\mathbf{a} \mid \mathbf{b} = \boldsymbol{\beta}$ is to begin by finding the conditional distribution $\mathcal{N}(\boldsymbol{\mu}_{\mathbf{a}|\boldsymbol{\beta}}, \boldsymbol{\Sigma}_{\mathbf{a},\mathbf{a}|\boldsymbol{\beta}})$. Having done so, we then construct a location-scale transform (1) by taking a square root of $\boldsymbol{\Sigma}_{\mathbf{a},\mathbf{a}|\boldsymbol{\beta}}$.

Due to their inherent emphasis, we refer to methods for representing (and generating) the random variable $\mathbf{a} \mid \mathbf{b} = \boldsymbol{\beta}$ by way of its corresponding conditional distribution $p(\mathbf{a} \mid \mathbf{b} = \boldsymbol{\beta})$ as being *distributional* in nature. This approach to conditioning is not only standard, but particularly natural when the quantity of interest may be derived analytically from $p(\mathbf{a} \mid \mathbf{b} = \boldsymbol{\beta})$. Often, however, quantities of interest such as expectations of nonlinear functions cannot be deduced analytically from $p(\mathbf{a} \mid \mathbf{b} = \boldsymbol{\beta})$ alone. This instead requires us to work with realizations of $\mathbf{a} \mid \mathbf{b} = \boldsymbol{\beta}$. In these cases then, we may be better off approaching Gaussian conditionals from a different perspective.

2.2 Pathwise conditioning

Instead of taking a *distribution-first* stance on Gaussian conditionals, we may think of conditioning directly in terms of random variables. In this *variable-first* paradigm, we will explicitly map from prior to posterior random variables and let the corresponding relationship

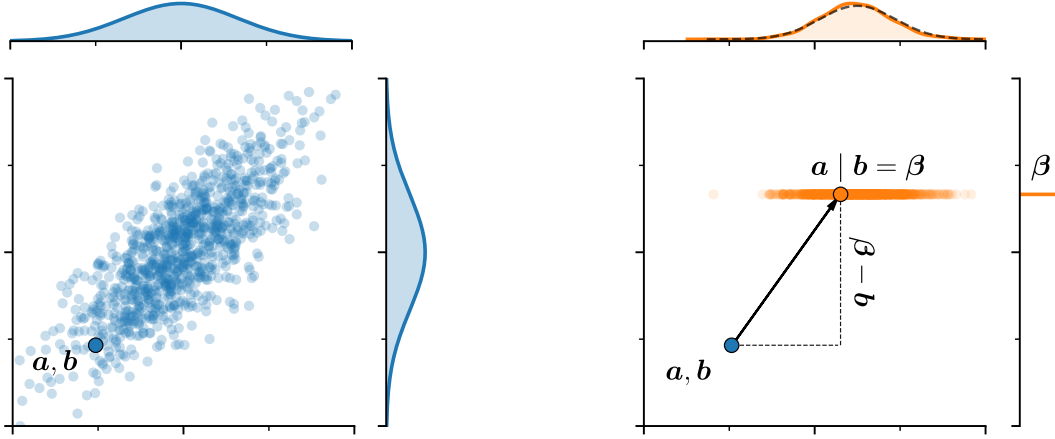


Figure 1: Visualization of Matheron’s update rule for a bivariate normal distribution with correlation coefficient $\rho = 0.75$. *Left*: Draws from $p(\mathbf{a}, \mathbf{b})$ are shown along with the marginal distributions. *Right*: Theorem 1 is used to update samples shown on the left subject to the condition $\mathbf{b} = \beta$. This process is illustrated in full for one a particular draw. *Top right*: the empirical distribution of the update samples is compared with $p(\mathbf{a} \mid \mathbf{b} = \beta)$.

between distributions follow implicitly. Throughout this work, we investigate this notion of *pathwise conditioning* through the lens of the following result.

Theorem 1 (Matheron’s Update Rule) *Let \mathbf{a} and \mathbf{b} be jointly Gaussian, centered random variables. Then the random variable \mathbf{a} conditional on $\mathbf{b} = \beta$ may be expressed as*

$$(\mathbf{a} \mid \mathbf{b} = \beta) \stackrel{d}{=} \mathbf{a} + \Sigma_{\mathbf{a}, \mathbf{b}} \Sigma_{\mathbf{b}, \mathbf{b}}^{-1} (\beta - \mathbf{b}). \quad (4)$$

Proof Comparing the mean and covariance on both sides immediately affirms the result

$$\begin{aligned} \mathbb{E}(\mathbf{a} + \Sigma_{\mathbf{a}, \mathbf{b}} \Sigma_{\mathbf{b}, \mathbf{b}}^{-1} (\beta - \mathbf{b})) &= \mu_{\mathbf{a}} + \Sigma_{\mathbf{a}, \mathbf{b}} \Sigma_{\mathbf{b}, \mathbf{b}}^{-1} (\beta - \mu_{\mathbf{b}}) \\ &= \mathbb{E}(\mathbf{a} \mid \mathbf{b} = \beta) \end{aligned} \quad \begin{aligned} \text{Cov}(\mathbf{a} + \Sigma_{\mathbf{a}, \mathbf{b}} \Sigma_{\mathbf{b}, \mathbf{b}}^{-1} (\beta - \mathbf{b})) &= \Sigma_{\mathbf{a}, \mathbf{a}} + \Sigma_{\mathbf{a}, \mathbf{b}} \Sigma_{\mathbf{b}, \mathbf{b}}^{-1} \text{Cov}(\mathbf{b}) \Sigma_{\mathbf{b}, \mathbf{b}}^{-1} \Sigma_{\mathbf{b}, \mathbf{a}} \\ &= \Sigma_{\mathbf{a}, \mathbf{a}} + \Sigma_{\mathbf{a}, \mathbf{b}} \Sigma_{\mathbf{b}, \mathbf{b}}^{-1} \Sigma_{\mathbf{b}, \mathbf{a}} = \text{Cov}(\mathbf{a} \mid \mathbf{b} = \beta). \end{aligned} \quad (5)$$

■

This observation leads to a simple recipe for simulating $\mathbf{a} \mid \mathbf{b} = \beta$: (i) sample $\mathbf{a}, \mathbf{b} \sim p(\mathbf{a}, \mathbf{b})$, and (ii) update the prior draw according to (4). In comparison to location-scale approach discussed in Section 2.1, a key difference here is that we now sample *before* conditioning, rather than after. Figure 1 visualizes the deterministic process of updating previously generated draws from the prior subject to the condition $\mathbf{b} = \beta$.

At first glance, Matheron’s update rule may seem like a lesser curio rather than a valuable tool. Indeed, the conventional strategy for sampling \mathbf{a}, \mathbf{b} (via a matrix square root of Σ) is more expensive than that for $\mathbf{a} \mid \mathbf{b} = \beta$. We will discuss this matter in detail in the following

sections. For now, however, we seek to strengthen our intuition by delving deeper into this expression's function-analytic origins.

2.3 Deriving pathwise conditioning via conditional expectations

Here, we overview the precise formalism that gives rise to the pathwise approach to conditioning Gaussian random variables and show how to *derive* this result from first principles. In short, we will show that Theorem 1 is a consequence of: (a) the linearity of Gaussian conditional expectations, (b) the projection theorem for Hilbert spaces, and (c) the independence of uncorrelated jointly Gaussian random variables.

We begin by recalling basic properties of conditional expectations. Let $(\Omega, \mathcal{F}, \mathbb{P})$ be a probability space and denote by (\mathbf{a}, \mathbf{b}) a pair of square integrable, centered random variables on $\mathbb{R}^{n_a} \times \mathbb{R}^{n_b}$. The conditional expectation is the unique random variable that minimizes the optimization problem¹

$$\mathbb{E}(\mathbf{a} \mid \mathbf{b}) = \arg \min_{\hat{\mathbf{a}} = f(\mathbf{b})} \mathbb{E}(\hat{\mathbf{a}} - \mathbf{a})^2. \quad (6)$$

In words then, $\mathbb{E}(\mathbf{a} \mid \mathbf{b})$ is the measurable function of \mathbf{b} that best predicts \mathbf{a} in the sense of minimizing the mean square error (6).

Uncorrelated, jointly Gaussian random variables are independent. Consequently, when \mathbf{a} and \mathbf{b} are jointly Gaussian, the optimal predictor $\mathbb{E}(\mathbf{a} \mid \mathbf{b})$ manifests as the *best unbiased linear estimator* $\hat{\mathbf{a}} = \mathbf{S}\mathbf{b}$ of \mathbf{a} (see Lemma 2). In this case then, the minimization problem (6) can be reinterpreted as the task of finding the optimal matrix $\mathbf{S} \in \mathbb{R}^{n_a \times n_b}$. At the same time, following the general theory of Hilbert spaces, we may interpret the problem of minimizing $\mathbb{E}(\mathbf{S}\mathbf{b} - \mathbf{a})^2$ as one of orthogonally projecting $\mathbf{a} \in L^2(\Omega, \mathcal{F}, \mathbb{P})$ —an element of the space of square integrable random variables—onto an appropriately chosen subspace.²

Putting these facts together, it follows that the *residuals* $\mathbf{r} = \mathbf{S}\mathbf{b} - \mathbf{a}$ induced by the optimal matrix \mathbf{S} must be orthogonal to every b_i in \mathbf{b} and, thus, to $\mathbf{S}\mathbf{b}$ as well. Here, *orthogonality* precisely coincides with *uncorrelatedness*. When \mathbf{a} is scalar, we may write³

$$(a \perp r) \iff 0 = \langle a, r \rangle_{L^2(\Omega, \mathcal{F}, \mathbb{P})} = \int_{\Omega} a(\omega)r(\omega) d\omega = \mathbb{E}(a \cdot r) = \text{Cov}(a, r). \quad (7)$$

By definition, the optimal \mathbf{S} satisfies $\text{Cov}(\mathbf{a} - \mathbf{S}\mathbf{b}, \mathbf{b}) = \boldsymbol{\Sigma}_{\mathbf{a}, \mathbf{b}} - \mathbf{S}\boldsymbol{\Sigma}_{\mathbf{b}, \mathbf{b}} = \mathbf{0}$. The following lemma presents the obvious solution to this problem and affirms the result.

Lemma 2 *For jointly Gaussian random variables $(\mathbf{a}, \mathbf{b}) \sim \mathcal{N}(\mathbf{0}, \boldsymbol{\Sigma})$, the conditional expectation of \mathbf{a} given \mathbf{b} is*

$$\mathbb{E}(\mathbf{a} \mid \mathbf{b}) = \boldsymbol{\Sigma}_{\mathbf{a}, \mathbf{b}} \boldsymbol{\Sigma}_{\mathbf{b}, \mathbf{b}}^{-1} \mathbf{b}. \quad (8)$$

Proof Let $\mathbf{S} \in \mathbb{R}^{n_a \times n_b}$ and $\mathbf{r} \in \mathbb{R}^{n_a}$ be defined as before and, by linearity, write

$$\mathbb{E}(\mathbf{a} \mid \mathbf{b}) = \mathbb{E}(\mathbf{S}\mathbf{b} + \mathbf{r} \mid \mathbf{b}) = \mathbb{E}(\mathbf{S}\mathbf{b} \mid \mathbf{b}) + \mathbb{E}(\mathbf{r} \mid \mathbf{b}). \quad (9)$$

1. Here, $f : \mathbb{R}^{n_b} \rightarrow \mathbb{R}^{n_a}$ runs through all Borel measurable functions—see Lemma 4.46 of Lord et al. (2014).

2. See Definition 4.47 and Example 4.51 of Lord et al. (2014), as well as Kallenberg (2006).

3. More generally, this equivalence is defined via centered inner products, see Rodgers et al. (1984).

From the definition of conditional expectation, we have $\mathbb{E}(\mathbf{S}\mathbf{b} \mid \mathbf{b}) = \mathbf{S}\mathbf{b}$, hence the first of the two terms on the left is immediately recognized to be $\Sigma_{\mathbf{a},\mathbf{b}}\Sigma_{\mathbf{b},\mathbf{b}}^{-1}\mathbf{b}$. For the second, (\mathbf{r}, \mathbf{b}) are jointly Gaussian, but uncorrelated: by independence, $\mathbb{E}(\mathbf{r} \mid \mathbf{b}) = \mathbb{E}(\mathbf{r}) = \mathbf{0}$. The result follows. \blacksquare

Having established insight for Gaussian conditional expectations, we now revisit Theorem 1.

Theorem 1 (Matheron’s Update Rule) *Let \mathbf{a} and \mathbf{b} be jointly Gaussian, centered random variables. Then the random variable \mathbf{a} conditional on $\mathbf{b} = \boldsymbol{\beta}$ may be expressed as*

$$(\mathbf{a} \mid \mathbf{b} = \boldsymbol{\beta}) \stackrel{\text{d}}{=} \mathbf{a} + \Sigma_{\mathbf{a},\mathbf{b}}\Sigma_{\mathbf{b},\mathbf{b}}^{-1}(\boldsymbol{\beta} - \mathbf{b}). \quad (4)$$

Proof Write

$$\mathbf{a} = \mathbb{E}(\mathbf{a} \mid \mathbf{b}) + (\mathbf{a} - \mathbb{E}(\mathbf{a} \mid \mathbf{b})), \quad (10)$$

where, as per the preceding derivation, residuals $(\mathbf{a} - \mathbb{E}(\mathbf{a} \mid \mathbf{b}))$ are independent of both \mathbf{b} and $\mathbb{E}(\mathbf{a} \mid \mathbf{b})$. Conditioning both sides of this expression on $\mathbf{b} = \boldsymbol{\beta}$ yields

$$(\mathbf{a} \mid \mathbf{b} = \boldsymbol{\beta}) \stackrel{\text{d}}{=} \mathbb{E}(\mathbf{a} \mid \mathbf{b} = \boldsymbol{\beta}) + (\mathbf{a} - \mathbb{E}(\mathbf{a} \mid \mathbf{b})), \quad (11)$$

where, on the right, the condition $\mathbf{b} = \boldsymbol{\beta}$ disappears from the second term by independence. Finally, evaluating both conditional expectations and simplifying gives the desired result

$$(\mathbf{a} \mid \mathbf{b} = \boldsymbol{\beta}) \stackrel{\text{d}}{=} \Sigma_{\mathbf{a},\mathbf{b}}\Sigma_{\mathbf{b},\mathbf{b}}^{-1}\boldsymbol{\beta} + (\mathbf{a} - \Sigma_{\mathbf{a},\mathbf{b}}\Sigma_{\mathbf{b},\mathbf{b}}^{-1}\mathbf{b}) = \mathbf{a} - \Sigma_{\mathbf{a},\mathbf{b}}\Sigma_{\mathbf{b},\mathbf{b}}^{-1}(\mathbf{b} - \boldsymbol{\beta}). \quad (12)$$

Hence, the claim follows. \blacksquare

In summary, we have shown that Matheron’s update rule is direct consequence of the fact that a Gaussian random variable \mathbf{a} conditioned on the outcome $\boldsymbol{\beta}$ of another (jointly) Gaussian random variable \mathbf{b} may be expressed as the sum of two independent terms: the conditional expectation $\mathbb{E}(\mathbf{a} \mid \mathbf{b} = \boldsymbol{\beta})$ and the residual $\mathbf{a} - \mathbb{E}(\mathbf{a} \mid \mathbf{b})$. Rearranging these terms gives (4).

With these ideas in mind and tools at hand, we are ready to explore this work’s primary theme: Matheron’s update rule enables us to decompose $\mathbf{a} \mid \mathbf{b} = \boldsymbol{\beta}$ into the prior random variable \mathbf{a} and an update term that explicitly corrects for the error in the coinciding value of \mathbf{b} given the condition $\mathbf{b} = \boldsymbol{\beta}$. Hence, Theorem 1 provides an explicit means of separating out the effects of the prior from those of the data. This *decoupling* is not possible in the distributional setting, since adding an arbitrary independent distribution to the prior cannot reduce our uncertainty. We thus proceed to investigate the ramifications of pathwise conditioning for Gaussian processes.

3. Conditioning Gaussian processes and random functions

A Gaussian process (GP) is a random function $f : \mathcal{X} \rightarrow \mathbb{R}$, such that, for any finite collection of points $\mathbf{X} \subset \mathcal{X}$, the random vector $\mathbf{f} = f(\mathbf{X})$ follows a multivariate Gaussian distribution.

In particular, if $f \sim \mathcal{GP}(\mu, k)$, then $\mathbf{f} \sim \mathcal{N}(\boldsymbol{\mu}, \mathbf{K})$ is multivariate normal with mean $\boldsymbol{\mu} = \mu(\mathbf{X})$ and covariance $\mathbf{K} = k(\mathbf{X}, \mathbf{X})$ specified by a kernel k .

Throughout this section, we investigate different ways of reasoning about conditional random variables $\mathbf{f}_* \mid \mathbf{f}_n = \mathbf{y}$ for some non-trivial partition $\mathbf{f} = \mathbf{f}_n \oplus \mathbf{f}_*$. Here, $\mathbf{f}_n = f(\mathbf{X}_n)$ and $\mathbf{f}_* = f(\mathbf{X}_*)$ denote (process values at) locations where we would like to introduce a condition $\mathbf{f}_n = \mathbf{y}$ and obtain a random variable $\mathbf{f}_* \mid \mathbf{f}_n = \mathbf{y}$, respectively. As in Section 2, we begin by reviewing distributional conditioning, before examining its pathwise counterpart.

3.1 Distributional conditioning

Like in finite-dimensional cases, we may obtain $\mathbf{f}_* \mid \mathbf{y}$ by first finding its conditional distribution. Since the process values $(\mathbf{f}_n, \mathbf{f}_*)$ are jointly Gaussian, this procedure closely resembles that of Section 2.1: we factor out the marginal distribution of \mathbf{f}_n from the joint distribution $p(\mathbf{f}_n, \mathbf{f}_*)$ and, upon canceling, identify the remaining distribution as $p(\mathbf{f}_* \mid \mathbf{y})$. Having done so, we find that the posterior distribution is the Gaussian $\mathcal{N}(\boldsymbol{\mu}_{*|n}, \mathbf{K}_{*,*|n})$ with moments

$$\boldsymbol{\mu}_{*|n} = \boldsymbol{\mu}_* + \mathbf{K}_{*,n} \mathbf{K}_{n,n}^{-1} (\mathbf{y} - \boldsymbol{\mu}_n) \quad \mathbf{K}_{*,*|n} = \mathbf{K}_{*,*} - \mathbf{K}_{*,n} \mathbf{K}_{n,n}^{-1} \mathbf{K}_{n,*}. \quad (13)$$

Assuming an inverse or Cholesky factor of $\mathbf{K}_{n,n}$ has already been computed, we may now proceed to generate $\mathbf{f}_* \mid \mathbf{y}$ at $\mathcal{O}(*^3)$ cost by using the location-scale transform (1)

This recipe for sampling from a Gaussian process posterior is subtly different from the one given in Section 2.1. Conditioning on $\mathbf{f}_n = \mathbf{y}$ does not change the fact that a Gaussian process is a distribution over functions. Owing to practical challenges for working with (conditional) distributions over infinite-dimensional objects however, distribution-based simulation of $\mathbf{f}_* \mid \mathbf{y}$ operates in terms of finite-dimensional marginals $\mathbf{f} = \mathbf{f}_n \oplus \mathbf{f}_*$. When quantities of interests are indeed defined over process values at a reasonable number (up to a few thousand) of predetermined locations \mathbf{X}_* , this approach to generating $\mathbf{f}_* \mid \mathbf{y}$ performs admirably. Increasingly, however, modern scientists require the flexibility afforded by working in terms of actual functions, such as the ability to efficiently evaluate and automatically differentiate $(f \mid \mathbf{y})(\mathbf{x}_*)$ at arbitrary locations $\mathbf{x}_* \in \mathcal{X}$. To this end, we now proceed to examine the direct approach to conditioning draws of $f \sim \mathcal{GP}(\mu, k)$.

3.2 Pathwise conditioning

Examining the pathwise update given by Theorem 1, it is natural to wonder whether the analogous statement holds for Gaussian processes. A quick check confirms this hypothesis.

Corollary 4 *For a Gaussian process $f \sim \mathcal{GP}(\mu, k)$ with marginal $\mathbf{f}_n = f(\mathbf{X}_n)$, the process conditioned on $\mathbf{f}_n = \mathbf{y}$ may be expressed as*

$$\underbrace{(f \mid \mathbf{y})(\cdot)}_{\text{conditional}} \stackrel{\text{d}}{=} \underbrace{f(\cdot)}_{\text{prior}} + \underbrace{k(\cdot, \mathbf{X}_n) \mathbf{K}_{n,n}^{-1} (\mathbf{y} - \mathbf{f}_n)}_{\text{update}}. \quad (14)$$

Proof Follows by applying Theorem 1 to an arbitrary set of locations. ■

Figure 2 acts a visual guide to Corollary 4. From left to right, we begin by generating a realization of $f \sim \mathcal{GP}(\mu, k)$ using methods discussed in Section 4. Having obtained a sample

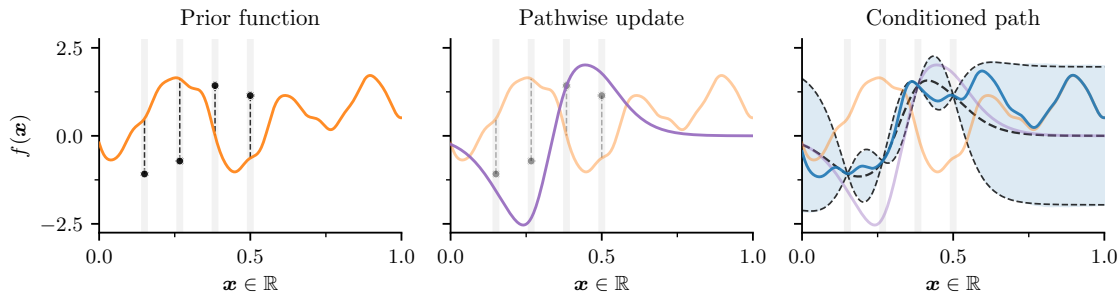


Figure 2: Visual overview for pathwise conditioning of Gaussian processes. *Left*: The residual $\mathbf{r} = \mathbf{y} - \mathbf{f}_n$ (dashed black) of a draw $f \sim \mathcal{GP}(0, k)$, shown in orange, given observations \mathbf{y} (black). *Middle*: A pathwise update (purple) is constructed in accordance with Corollary 4. *Right*: Prior and update are combined to represent conditional (blue). Empirical moments (light blue) of 10^5 conditioned paths are compared with those of the model (dashed black). The sample average, which matches the posterior mean, has been omitted for clarity.

path, we then use the pathwise update (14) to define a function $k(\cdot, \mathbf{X}_n)\mathbf{K}_{n,n}(\mathbf{y} - \mathbf{f}_n)$ to explain for residual $\mathbf{y} - \mathbf{f}_n$. Adding these two functions together produces a draw from GP posterior, behavior of which is shown on the right.

Whereas the location-scale representation for (marginals of) conditional GPs discusses random vectors, (14) is a statement about *random functions*. This paradigm shift echoes our primary message: Gaussian (process) conditionals can be understood directly in terms of random variables. In turn, we argue that Corollary 4 significantly impacts *how* we think about Gaussian process posteriors and, therefore, *what* we do with them.

Having said this, there are several hurdles that we must overcome in order to use the pathwise update (14) in the real world. First, we are typically unable to practically sample functions $f \sim \mathcal{GP}(\mu, k)$ from (non-degenerate) Gaussian process priors exactly. Algorithmically, complicated functions $f(\cdot)$ can be represented by combining elementary functions $\phi_i(\cdot)$ using a given set of algebraic operations. When the requisite number of elementary functions is infinite however, evaluating $f(\cdot)$ is usually impossible. In Section 4, we will therefore investigate different ways of approximating $f(\cdot)$ using a finite number of operations.

Second, naïve use of (14) incurs $\mathcal{O}(n^3)$ time complexity owing to the need to solve the linear system of equations $\mathbf{K}_{n,n}\mathbf{v} = \mathbf{y} - \mathbf{f}_n$ in order to obtain a vector $\mathbf{v} \in \mathbb{R}^n$, such that

$$(f | \mathbf{y})(\cdot) \stackrel{d}{=} f(\cdot) + \sum_{i=1}^n v_i k(\cdot, \mathbf{x}_i). \quad (15)$$

Here, we have re-expressed the matrix-vector product in (14) as an expansion with respect to the canonical basis functions $k(\cdot, \mathbf{x}_i)$ centered at training locations $\mathbf{x}_i \in \mathbf{X}_n$. For large training sets $(\mathbf{X}_n, \mathbf{y})$ then, direct application of (14) may prove prohibitively expensive. By the same token, the stated pathwise update does not hold when outcomes \mathbf{y} are not defined as realizations of process values \mathbf{f}_n . We consider various means of resolving these challenges, and ones like them, in Section 5.

3.3 Historical remarks

Prior to continuing, we pause to reflect on the historical developments that have paved the way for this work. In a 2005 tribute to geostatistics pioneer Georges Matheron, Chilès and Lantuéjoul (2005) comment that

[Matheron’s update rule] is nowhere to be found in Matheron’s entire published works, as he merely regarded it as an immediate consequence of the orthogonality of the [conditional expectation] and the [residual process].

As if to echo this very sentiment, Doucet (2010) begins a much appreciated technical note on the subject of Theorem 1 with the humorous remark

This note contains no original material and will never be submitted anywhere for publication. However it might be of interest to people working with Gaussian random fields/processes so I am making it publicly available.

The presiding opinion therefore seems to be that Matheron’s update rule is too simple to warrant extended study. Indeed, Theorem 1 is straightforward to verify. As is often the case however, this result is significantly harder to discover if one is not already aware of its existence. The dilemma may help to explain why Matheron’s update rule is absent from standard machine learning texts. By deriving this result from first principles in Section 2.3, we hope to encourage fellow researchers to explore the strengths (and weaknesses) of the pathwise viewpoint espoused here.

Having said this, we are not the first to have realized the practical implications of pathwise conditioning for GPs. Corollary 4 is relatively well-known in geostatistics (Journel and Huijbregts, 1978; de Fouquet, 1994; Emery, 2007; Chiles and Delfiner, 2009). Along the same lines, Oliver (1996) discusses Matheron’s update rule for Gaussian likelihoods (Section 5.1). Similar ideas were rediscovered in the 1990s with applications to astrophysics. In particular, Hoffman and Ribak (1991) propose the use spectral approximations to stationary priors (Section 4.2) in conjunction with the canonical pathwise update (15).

At the same time, these formulae are seldom seen in machine learning. We hope to systematically organize these findings (along with our own) and communicate them to a general audience of machine learners, theorists, and practitioners.

4. Sampling functions from Gaussian process priors

The pathwise representation of GP posteriors described in the preceding section allows us to generate $f \mid \mathbf{y}$ by transforming a draw of $f \sim \mathcal{GP}(0, k)$. In order for such a method to be deemed *efficient*, we therefore require that both realizing the prior function and performing the update scale appreciably in the total number of locations $\mathbf{X} = \mathbf{X}_n \oplus \mathbf{X}_*$. Half of the battle is, therefore, to obtain faithful but affordable draws f . Fortunately, GP priors often exhibit convenient mathematical properties not present in their posteriors, which can be utilized to sample them efficiently.

We focus on strategies for generating random *functions* that we may evaluate at arbitrary locations $x \in \mathcal{X}$ in $\mathcal{O}(1)$ time and whose marginal distributions approximate those of $f \sim \mathcal{GP}(0, k)$. Conceptually, techniques discussed here approximate prior draws as weighted

combinations of a finite number of suitably chosen basis functions $\phi = (\phi_1, \dots, \phi_\ell)$ given by

$$f^{(w)}(\cdot) = \sum_{i=1}^{\ell} w_i \phi_i(\cdot) \quad \mathbf{w} \sim \mathcal{N}(\mathbf{0}, \Sigma_{\mathbf{w}}), \quad (16)$$

where the covariance of the Gaussian random weight vector \mathbf{w} will vary by case. We stress that, for any sample of weights \mathbf{w} , the corresponding realization of $f^{(w)}$ acts as a typical function would. In particular, we incur $\mathcal{O}(1)$ cost for evaluating $f^{(w)}(\mathbf{x})$. Moreover, we may readily differentiate $f^{(w)}$ with respect to \mathbf{x} or other parameters of interest.

At the same time, $f^{(w)}$ itself is a random function satisfying $\mathbf{f}^{(w)} \sim \mathcal{N}(\mathbf{0}, \Phi_n \Sigma_{\mathbf{w}} \Phi_n^\top)$, where $\Phi_n = \phi(\mathbf{X})$ is a $|\mathbf{X}| \times \ell$ matrix of features. By design then, $f^{(w)}$ is a Gaussian process. In machine learning, (16) is commonly known as the *weight-space* view of GPs (Rasmussen and Williams, 2006).

Below, we identify different ℓ -dimensional bases ϕ_i such that $f \stackrel{\text{d}}{\approx} f^{(w)}$. Additionally, we will require that a matrix square root of $\Sigma_{\mathbf{w}}$ can be cheaply obtained, such that \mathbf{w} may be efficiently generated via a location-scale transform (1). Our presentation is intended to shed light on different approaches to finding suite bases ϕ_i and is by no means exhaustive. In order to set the scene for these approximate priors, we begin by recounting properties of the gold standard: location-scale methods.

4.1 Exact methods

Location-scale methods (1) are the most widely used approach for generating Gaussian random vectors. This generative strategy is *exact* (up to machine precision). Given locations \mathbf{X} , we may simulate $\mathbf{f} = f(\mathbf{X})$ in location-scale fashion as

$$\mathbf{f}(\mathbf{X}) \stackrel{\text{d}}{=} \mathbf{K}^{1/2} \boldsymbol{\zeta} \quad \boldsymbol{\zeta} \sim \mathcal{N}(\mathbf{0}, \mathbf{I}) \quad (17)$$

by multiplying a square root covariance matrix $\mathbf{K}^{1/2}$ by a standard normal vector $\boldsymbol{\zeta}$. Especially when $|\mathbf{X}|$ is large, popular recipes for obtaining $\mathbf{K}^{1/2}$, such as the Cholesky factorization, may fail due to \mathbf{K} being ill-conditioned. In practice, this issue is typically circumvented by instead taking a square root of the *jittered* covariance matrix $\mathbf{K} + \epsilon \mathbf{I}$, where $\epsilon > 0$ is a small positive constant (typically on the order of 10^{-6}). This fix introduces a small but non-zero amount of additional error.

While (17) is rightly seen as the method of choice for many problems, it is not without shortcoming. Chief among these issues is the fact that algorithms for obtaining a matrix square root of \mathbf{K} scale cubically in $|\mathbf{X}|$. In most cases, this limits the use of location-scale approaches to cases where the length of the desired Gaussian random vector is modest (up to a few thousand). This overhead can be interpreted to mean that we incur $\mathcal{O}(i^2)$ cost for generating the i -th element of \mathbf{f} , which leads us to our second issue: reusing a previously generated draw of \mathbf{f}_n (and other previously computed terms) to more efficiently generate \mathbf{f} requires us to sample from the conditional distribution

$$\mathbf{f}_* \mid \mathbf{f}_n \sim \mathcal{N}(\boldsymbol{\mu}_* + \mathbf{K}_{*,n} \mathbf{K}_{n,n}^{-1} (\mathbf{f}_n - \boldsymbol{\mu}_n), \mathbf{K}_{*,*} - \mathbf{K}_{*,n} \mathbf{K}_{n,n}^{-1} \mathbf{K}_{n,*}). \quad (18)$$

The asymptotic cost for drawing the random vector \mathbf{f} is still cubic in its the length, however, the actual time taken to generate \mathbf{f} increases. When locations \mathbf{x} in \mathbf{X} are defined online

rather than in advance however, (location-scale-based) alternatives for generating \mathbf{f} are few and far between. Further refining this predicament we arrive at our final challenge: pathwise derivatives.

Since differentiation is a linear operation, the gradient of a Gaussian process f with respect to \mathbf{x} is another Gaussian process. By construction, these GPs are correlated. Hence, if we are interested in using gradient information to, say, efficiently identify a local minimizer $\mathbf{x}_{\min} \in \mathcal{X}$ of a sample path, we must re-condition both processes on samples of $f(\mathbf{x}_t)$ and $\nabla f(\mathbf{x}_t)$ with each passing step t of gradient descent.

In select cases, the otherwise cubic costs for computing a square root in (17) can be dramatically reduced by exploiting structural assumptions regarding covariance matrices \mathbf{K} . Well-known examples of this trend include banded and sparse matrices in the context of one-dimensional Gaussian processes and Gauss–Markov random fields (Rue and Held, 2005; Loper et al., 2020; Durrande et al., 2019), as well as Kronecker and Toeplitz matrices when working with regularly-spaced grids $\mathbf{X} \in \mathcal{X}$ (Dietrich and Newsam, 1997; Chan and Wood, 1997), and kernel interpolation methods (Wilson and Nickisch, 2015; Pleiss et al., 2018). When the chosen covariance function or application allows it, these methods are highly effective. We now proceed to explore methods that avoid these issues by approximating Gaussian process priors as Bayesian linear models.

4.2 Stationary covariances

Stationary covariance functions $k(\mathbf{x}, \mathbf{x}') = k(\mathbf{x} - \mathbf{x}')$, such as the Matérn family’s squared exponential kernel, give rise to a significant option of GP priors in use today. For centered Gaussian process priors $f \sim \mathcal{GP}(0, k)$, stationarity encodes the belief that the relationship between process values $f(\mathbf{x}_i)$ and $f(\mathbf{x}_j)$ is not affected by the simultaneous translation of the corresponding locations \mathbf{x}_i and \mathbf{x}_j . Owing to its combination of simplicity and modeling flexibility, this assumption is often the initial choice considered in many applied problems.

These kernels exhibit a variety of special properties that greatly facilitate the construction of efficient prior approximations. Here, we restrict attention to kernels admitting a spectral density ρ , and focus on the class of estimators formed by discretizing the spectral representation of k

$$k(\mathbf{x} - \mathbf{x}') = \int_{\mathbb{R}^d} e^{2\pi i \boldsymbol{\omega}^\top (\mathbf{x} - \mathbf{x}')} \rho(\boldsymbol{\omega}) d\boldsymbol{\omega} \quad \rho(\boldsymbol{\omega}) = \int_{\mathbb{R}^d} e^{-2\pi i \boldsymbol{\omega}^\top \mathbf{x}} k(\mathbf{x}) d\mathbf{x}. \quad (19)$$

By the *kernel trick* (Schölkopf and Smola, 2001), a kernel k can be written as the inner product in a corresponding reproducing kernel Hilbert space (RKHS) \mathcal{H}_k with a feature map $\varphi : \mathcal{X} \rightarrow \mathcal{H}_k$. In many cases, the aforementioned inner product can be approximated by

$$k(\mathbf{x}, \mathbf{x}') = \langle \varphi(\mathbf{x}), \varphi(\mathbf{x}') \rangle_{\mathcal{H}_k} \approx \boldsymbol{\phi}(\mathbf{x})^\top \overline{\boldsymbol{\phi}(\mathbf{x}')} \quad (20)$$

where $\boldsymbol{\phi} : \mathcal{X} \rightarrow \mathbb{C}^\ell$ is some finite-dimensional feature map and $\overline{\boldsymbol{\phi}(\mathbf{x}')}$ denotes the complex conjugate. Based on this idea, the method of *random Fourier features* (Rahimi and Recht, 2008) constructs a Monte Carlo estimate to a stationary kernel by representing the right-hand side of (20) in terms of ℓ complex exponential basis functions $\phi_j(\mathbf{x}) = \ell^{-1/2} \exp(i\boldsymbol{\omega}_j^\top \mathbf{x})$ with parameters $\boldsymbol{\omega}_j$ sampled proportional to the corresponding spectral density $\rho(\boldsymbol{\omega}_j)$.⁴

4. Using elementary trigonometric identities, we may also derive an related family of basis functions $\phi : \mathcal{X} \mapsto \mathbb{R}^\ell$ with $\phi_j(\mathbf{x}) = \sqrt{2/\ell} \cos(\boldsymbol{\omega}_j^\top \mathbf{x} + \tau_j)$ where $\tau_j \sim \mathcal{U}(0, 2\pi)$.

Given a set of basis functions ϕ_1, \dots, ϕ_ℓ , we may now proceed to approximate the true prior according to the Bayesian linear model

$$f^{(w)}(\cdot) = \sum_{i=1}^{\ell} w_i \phi_i(\cdot) \quad w_i \sim \mathcal{N}(0, 1). \quad (21)$$

Under this approximation, $f^{(w)}$ is a random function satisfying $\mathbf{f}_n^{(w)} \sim \mathcal{N}(\mathbf{0}, \mathbf{\Phi}_n \mathbf{\Phi}_n^\top)$, where $\mathbf{\Phi}_n = \phi(\mathbf{X}_n)$ is an $n \times \ell$ matrix of features. By design then, $f^{(w)}$ is a Gaussian process whose covariance approximates that of f .

The random Fourier feature approach is particularly appealing since its formulation as a Monte Carlo estimator causes the error introduced by the ℓ -dimensional basis ϕ_i decays at the *dimension-free* rate $\ell^{-1/2}$ (Sutherland and Schneider, 2015). This property enables us to balance accuracy and cost by choosing the value ℓ that best suites our needs.

4.3 Karhunen–Lo  ve expansions

To the extent that it may be the most widely used, stationarity is not the only property that we may avail ourselves of when seeking to emulate GP priors via finite-dimensional bases. We now consider another approach to constructing approximate function draws: the *Karhunen–Lo  ve expansion* (Castro et al., 1986; Fukunaga, 2013).

To motivate this expansion, consider the family of ℓ -dimensional Bayesian linear model $f^{(w)}(\cdot) = \phi(\cdot)^\top \mathbf{w}$ consisting of orthonormal basis functions $\phi_i : \mathcal{X} \rightarrow \mathbb{R}$ on a compact space \mathcal{X} . Following standard theory (Fukunaga, 2013), the *optimal* $f^{(w)}$ for approximating a Gaussian process f , in the sense of minimizing mean square error, is found by truncating the Karhunen–Lo  ve expansion

$$f(\cdot) = \sum_{i=1}^{\infty} w_i \phi_i(\cdot) \quad w_i \sim \mathcal{N}(0, \lambda_i) \quad (22)$$

where ϕ_i and λ_i are, respectively, the i -th eigenfunction and eigenvalue of the covariance operator $\psi \mapsto \int_{\mathcal{X}} \psi(\mathbf{x}) k(\mathbf{x}, \cdot) d\mathbf{x}$, written in decreasing order of λ_i .

Truncated versions of this expansion are used both as a technique for optimally approximating GPs (Zhu et al., 1997; Solin and S  rkk  , 2020), and as a modeling tool in their own right (Krainski et al., 2018). In most cases, eigenfunctions ϕ_i are either obtained by first principles (Krainski et al., 2018) or by numerical methods (Lindgren et al., 2011; Lord et al., 2014; Solin and Kok, 2019).

In addition to being optimal, Karhunen–Lo  ve expansions are highly general. Even when a covariance function k is non-stationary or the domain \mathcal{X} is non-Euclidean—such as when Gaussian processes are used to represent functions on manifolds (Borovitskiy et al., 2020b) and graphs (Borovitskiy et al., 2020a)—the Karhunen–Lo  ve expansion exists. The primary difficulty for using these truncated eigensystems is that, save for in rare case, they do not admit a convenient, analytic form. Efficient, numerical methods for obtaining (22) typically require us to utilize mathematical properties of the chosen kernel. These properties are often closely related to the differential-equation-based perspectives of Gaussian processes introduced in the following section.

4.4 Stochastic partial differential equations

Many Gaussian process priors, such as the Matérn family, can be expressed as solutions of *stochastic partial differential equations* (SPDEs). These equations also often arise in physics, where they describe a variety of phenomena, such as diffusion and heat transfer, that are deeply connected with the widely used squared exponential kernel (Grigoryan, 2009). Moreover, they are often a starting point for designing non-stationary GP priors (Krainski et al., 2018). We now describe how to construct basis-function representations of GP priors which admit such representations, using the *finite element method* for SPDEs (Evans, 2010; Lindgren et al., 2011; Lord et al., 2014).

Suppose a Gaussian process $f \sim \mathcal{GP}(0, k)$ satisfies $\mathcal{L}f = \mathcal{W}$, where \mathcal{L} is a linear differential operator and \mathcal{W} is a white noise process (Lifshits, 2012). We demonstrate how to derive a Gaussian process $f^{(w)}$ that approximately satisfies this SPDE. To begin, we express $\mathcal{L}f = \mathcal{W}$ in its corresponding weak form⁵

$$\int_{\mathcal{X}} (\mathcal{L}f)(\mathbf{x})g(\mathbf{x}) d\mathbf{x} = \int_{\mathcal{X}} g(\mathbf{x}) d\mathcal{W}(\mathbf{x}) \quad (23)$$

where g is an arbitrary element taken from an appropriate class of test functions. From here, we proceed by approximating both the desired solution f and the test function g with respect to the finite-dimensional basis ϕ_1, \dots, ϕ_ℓ as $f^{(w)}(\cdot) = \sum_{i=1}^{\ell} w_i \phi_i(\cdot)$ and $g^{(v)}(\cdot) = \sum_{j=1}^{\ell} v_j \phi_j(\cdot)$. Substituting these terms into (23) and differentiating both sides with respect to the coefficients of $g^{(v)}$, we obtain ℓ expressions, one for each $j = 1, \dots, \ell$,

$$\sum_{i=1}^{\ell} w_i \underbrace{\int_{\mathcal{X}} (\mathcal{L}\phi_i)(\mathbf{x})\phi_j(\mathbf{x}) d\mathbf{x}}_{A_{ij}} = \underbrace{\int_{\mathcal{X}} \phi_j(\mathbf{x}) d\mathcal{W}(\mathbf{x})}_{b_j}. \quad (24)$$

Defining $\mathbf{M} = \text{Cov}(\mathbf{b})$ where $\text{Cov}(b_i, b_j) = \langle \phi_i, \phi_j \rangle$ coincides with the finite-element mass matrix, we may now rearrange this system of random linear equations in matrix-vector form by writing $\mathbf{A}\mathbf{w} = \mathbf{b}$. The basis coefficients of the random function $f^{(w)}$ are then distributed as $\mathbf{w} \sim \mathcal{N}(\mathbf{0}, \mathbf{A}^{-1}\mathbf{M}\mathbf{A}^{-1})$. As in the previous sections, $f^{(w)}$ can be seen as the weight-space view of a corresponding Gaussian process.

A popular choice is to employ compactly supported basis functions ϕ_i . The matrices \mathbf{A} and \mathbf{M} are then sparse, and the resulting linear systems can be solved efficiently. By way of example, the family of *piecewise linear* basis functions is a particularly simple but effective choice for second order differential operators \mathcal{L} (Evans, 2010; Lord et al., 2014).⁶

4.5 Discussion

Each of the techniques described above provides a different means of obtaining a finite-dimensional Bayesian linear model $f^{(w)}$ that approximates a Gaussian process f . These

5. If necessary or desirable due to specific properties of the basis ϕ_i , we integrate $(\mathcal{L}f)(\mathbf{x})g(\mathbf{x})$ by parts—to simplify presentation, we suppress this from the notation.
 6. A second order differential operator gives rise to a first-order bilinear form when integrated by parts, which matches with piecewise linear basis functions which are once differentiable almost everywhere. For higher-order operators, a piecewise polynomial basis can be used instead.

models often behave in qualitatively distinct ways and achieve different balances of accuracy versus cost in different problems.

Fourier feature and Karhunen–Loève bases are *global*: each basis function helps to characterize the behavior of a random function $f^{(w)}$ over the entire domain \mathcal{X} . In contrast, *local* basis functions, such as the piecewise linear ones considered in Section 4.4, decay to zero away from some $\mathbf{x} \in \mathcal{X}$. Finite-dimensional local bases, therefore, typically provide rich information about a function’s behavior over restricted subsets of \mathcal{X} , but little elsewhere. For common choices of kernel k , the canonical basis functions $k(\cdot, \mathbf{x})$ featured in (15) constitute one such local basis.

This line of reasoning also helps to explain why random Fourier features have been observed to struggle at representing GP posteriors (Wang et al., 2018; Mutny and Krause, 2018; Calandriello et al., 2019). Note that, like the Karhunen–Loève basis functions, the complex exponentials can be interpreted as the eigenfunctions of stationary kernels (Rasmussen and Williams, 2006). Accordingly, we see that these global bases are effective at representing the prior. This result does not imply, however, that a given ℓ -dimensional basis ϕ is well-suited for representing process values at training locations \mathbf{X}_n .

In light of these trends, we generally prefer to use global basis functions to represent the prior and local basis functions to represent the effects of the data. On that note, let us now consider different ways of representing different types of data.

5. Conditioning via pathwise updates

Building off of the foundation prepared in Section 3, we now explore how Corollary 4 may be adapted to accommodate different forms of data-dependency and approximated to reduce computational overheads. Throughout this section, we use $\hat{\mathbf{y}}$ to denote the random variable that the observations \mathbf{y} realize under the given likelihood.

5.1 Gaussian updates

In Corollary 4, observations \mathbf{y} are treated as realized process values $\mathbf{f}_n = f(\mathbf{X}_n)$. Conditions therefore manifest as the equality constraint $\mathbf{f}_n = \mathbf{y}$. In the real world, however, \mathbf{y} is often contaminated by some degree of noise. Weaker conditions, compared to exact equality, are therefore required in order to separate out signal from noise. For this reason, it is common to interpret \mathbf{y} in terms of the Gaussian likelihood $p(\mathbf{y} \mid f(\mathbf{x})) = \mathcal{N}(f(\mathbf{x}), \sigma_\varepsilon^2)$. Following Theorem 1, we may condition the Gaussian process f on noisy observations \mathbf{y} , in pathwise fashion, as

$$(f \mid \mathbf{y})(\cdot) \stackrel{\text{d}}{=} f(\cdot) + k(\cdot, \mathbf{X})(\mathbf{K}_{n,n} + \sigma_\varepsilon^2 \mathbf{I})^{-1}(\mathbf{y} - \mathbf{f}_n - \varepsilon), \quad (25)$$

where the noise variable $\varepsilon \sim \mathcal{N}(\mathbf{0}, \sigma_\varepsilon^2 \mathbf{I})$ is such that $\hat{\mathbf{y}} \stackrel{\text{d}}{=} \mathbf{f}_n + \varepsilon$ under the given likelihood. The conditioned path $f \mid \mathbf{y}$ now interpolates between, rather than exactly passing through, observations \mathbf{y} .

5.2 Non-Gaussian updates

In the general setting, where the random variable $\hat{\mathbf{y}}$ is arbitrarily distributed under the likelihood, the outcome variables $\hat{\mathbf{y}}$ relate to process values \mathbf{f} by way of the non-conjugate

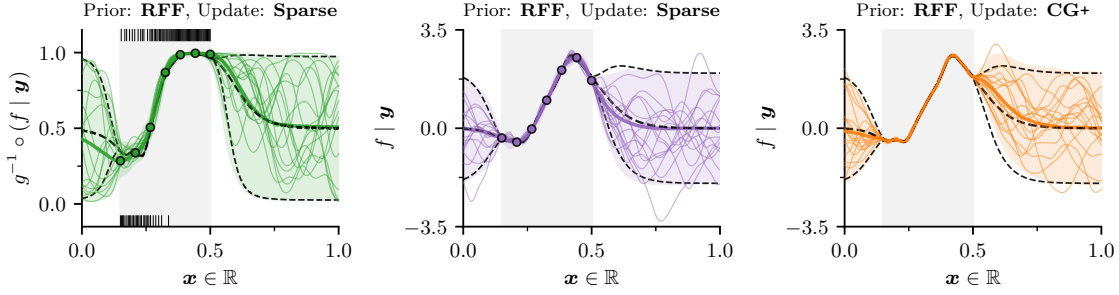


Figure 3: Visual comparison of different pathwise updates. *Left and middle:* Variational inference is used to learn sparse updates at $m = 7$ inducing locations \mathbf{Z} (circles). *Right:* conjugate gradients is used to approximately solve for a Gaussian update, “CG+” denotes use of the preconditioner proposed by Gardner et al. (2018). In all cases, 1000 observations y are evenly spaced in the shaded region and asymptotic costs of the updates are matched. Dashed lines denote mean and two standard deviations of ground truth posteriors, colored regions and thicker lines denote those of empirical ones. Middle and right plots illustrate regression with a Gaussian likelihood, the left plot shows binary classification with a Bernoulli likelihood and probit link function g . Every tenth label is shown as a bar.

prior

$$p(\hat{\mathbf{y}}, \mathbf{f}) = p(\hat{\mathbf{y}} | g^{-1}(\mathbf{f}_n)) \mathcal{N}(\mathbf{f} | \boldsymbol{\mu}, \mathbf{K}) \quad (26)$$

where $g : [0, 1] \rightarrow \mathbb{R}$ is known as the *link function*. For binary classification problems, popular choice for g include the logit and probit functions (Rasmussen and Williams, 2006). The left column of Figure 3 illustrates this scenario using methods described below.

Given (26), it remains the case that the conditional expectation of f given $\hat{\mathbf{y}} = \mathbf{y}$ and its corresponding residual are uncorrelated. However, since $p(\mathbf{f}, \hat{\mathbf{y}})$ may not be Gaussian, it no longer follows that this lack of correlation implies independence—hence, the pathwise update (14) does not hold. These cases emerge when working with non-conjugate priors and result in exact Bayesian inference and prediction becoming intractable.

Strategies for circumventing this issue generally approximate the true posterior by introducing an auxiliary random variable $\mathbf{u} \sim q(\mathbf{u})$ such that $f | \mathbf{u}$ resembles $f | \mathbf{y}$ according to a chosen measure of similarity (Nickisch and Rasmussen, 2008; Hensman et al., 2015). As a pragmatic assumption, \mathbf{u} is typically assumed to be jointly Gaussian with \mathbf{f} .⁷ Consequently, non-conjugate priors $p(\mathbf{f}, \hat{\mathbf{y}})$ are supplanted by conjugate ones $q(\mathbf{f}, \mathbf{u})$, whereupon Matheron’s update rule holds once more. The following section explores these *sparse* approximations in greater detail.

5.3 Sparse updates

Often, the need arises to condition a process f on a fictitious variable $\mathbf{u} = (u_1, \dots, u_m) \in \mathbb{R}^m$. Continuing from the previous section, the outcome variables $\hat{\mathbf{y}}$ may be non-Gaussian (Titsias and Lawrence, 2010; Damianou and Lawrence, 2013). Alternatively, the $\mathcal{O}(n^3)$ cost for

7. Note that, in the special case where $p(\mathbf{f}, \hat{\mathbf{y}})$ is Gaussian, the optimal q is also Gaussian (Titsias, 2009).

inverting $\mathbf{K}_{n,n}$ may be prohibitive (Titsias, 2009; Hensman et al., 2013). In these cases and more, we would like to infer a distribution $q(\mathbf{u})$ such that $f \mid \mathbf{u}$ explains for the data. Redefining the problem of updating f in this way not only avoids potential issues arising from non-Gaussianity of $\hat{\mathbf{y}}$, but associates the computational cost of conditioning with \mathbf{u} . As we will soon see, this yields pathwise updates with $\mathcal{O}(m^3)$ rather than $\mathcal{O}(n^3)$ runtime complexity.

Comprehensive treatment of approaches to learning an optimal distribution $q(\mathbf{u})$ is beyond the scope of this work. In general, however, these procedures operate by finding an approximate posterior $q(\mathbf{f}, \mathbf{u})$ within a tractable family of approximating distributions \mathcal{Q} . For reasons that will soon become clear, this family of distributions typically includes an additional set of parameters \mathbf{Z} , which help to define the joint distribution $p(\mathbf{f}, \mathbf{u})$. To help streamline presentation, we focus on the simplest and most widely used abstraction for inducing variables, namely *pseudo-data*.

In the pseudo-data framework (Snelson and Ghahramani, 2006; Quinonero-Candela et al., 2007; Titsias, 2009), $\mathbf{u} \sim q(\mathbf{u})$ assumes the role of process values $\mathbf{f}_m = f(\mathbf{Z})$ at free locations $\mathbf{Z} \in \mathcal{X}^m$. This paradigm gets its name from the intuition that the (random) collection of pseudo-data $(\mathbf{z}_j, u_j)_{j=1}^m$ which mimic the effect of the true data $(\mathbf{x}_i, y_i)_{i=1}^n$ on f . By construction, \mathbf{u} is jointly Gaussian with f .⁸ The desired pathwise update is then

$$(f \mid \mathbf{u})(\cdot) \stackrel{\text{d}}{=} f(\cdot) + \underbrace{\sum_{i=1}^m v_i k(\cdot, \mathbf{z}_i)}_{m\text{-dimensional basis}}, \quad (27)$$

where $\mathbf{v} = \mathbf{K}_{m,m}^{-1}(\mathbf{u} - \mathbf{f}_m)$. This formula is identical the one given by Corollary 4, save for the fact that we now sample $\mathbf{u} \sim q(\mathbf{u})$ and solve for a linear system involving the $m \times m$ covariance matrix $\mathbf{K}_{m,m} = k(\mathbf{Z}, \mathbf{Z})$ at $\mathcal{O}(m^3)$ cost. The middle column of Figure 3 illustrates the sparse update induced by Gaussian $\mathbf{u} \sim \mathcal{N}(\boldsymbol{\mu}_u, \boldsymbol{\Sigma}_u)$ with a learned distribution.

Similar to methods discussed in Section 4, we may think of (27) as approximating a function defined in terms of the n -dimensional basis $k(\cdot, \mathbf{X}_n)$ with respect to the m -dimensional basis $k(\cdot, \mathbf{Z})$. This basis is often efficient because training locations \mathbf{x} in \mathbf{X}_n in near proximity give rise to similar basis functions. Kernel basis functions at appropriately chosen sets of $m \ll n$ locations \mathbf{Z} exploit this redundancy to produce a sparser, more cost-efficient representation.

5.4 Iterative solvers

So far, we have focused on the high-level properties of pathwise updates in relation to various problem settings. This is to say nothing, however, of the explicit means by which we carry out such an update. In all cases discussed here, pathwise conditioning has revolved around solving a system of linear equations, e.g., $\mathbf{K}_{n,n}\mathbf{v} = \mathbf{y} - \mathbf{f}_n$ for coefficients \mathbf{v} , which combine with cross-covariance $k(\cdot, \mathbf{X}_n)$ to define the change in f subject to the condition $\mathbf{f}_n = \mathbf{y}$. Given a reasonable number of conditions n (up to a few thousand), we may obtain \mathbf{v} by first computing the Cholesky factor $\mathbf{L}_{n,n} = \mathbf{K}_{n,n}^{1/2}$ and then solving for a pair of triangular

8. More generally, this condition holds if \mathbf{u} relates to f by way of a linear map (Lázaro-Gredilla and Figueiras-Vidal, 2009).

systems $\mathbf{L}_{n,n}\bar{\mathbf{v}} = \mathbf{u} - \mathbf{f}_n$ and $\mathbf{L}_{n,n}^\top \mathbf{v} = \bar{\mathbf{v}}$. For large n however, the $\mathcal{O}(n^3)$ time complexity for enacting this recipe is typically prohibitive.

Rather than solving for coefficients \mathbf{v} directly, we may instead employ an *iterative solver*, which constructs a sequence of estimates $\mathbf{v}^{(1)}, \mathbf{v}^{(2)}, \dots$ to \mathbf{v} , such that $\mathbf{v}^{(j)}$ converges to the true \mathbf{v} as j increases. Depending on the numerical properties of the linear system to be solved, it's possible that a high-quality approximate solution $\mathbf{v}^{(j)}$ may be obtained after the j -th iteration for some $j \ll n$. This line of reasoning features prominently in a number of recent works, where iterative solvers have been shown to be a highly competitive approach to approximating GP posteriors (Pleiss et al., 2018; Gardner et al., 2018; Wang et al., 2019). The right column of Figure 3 visualizes an approximate solution of the Gaussian pathwise update (25) using preconditioned conjugate gradients (Gardner et al., 2018).

In these cases, posterior sampling via pathwise conditioning enjoys an important advantage over distributional approaches: it allows us to solve for linear system of the form $\mathbf{K}_{n,n}^{-1}\mathbf{v}$ rather than $\mathbf{K}_{*,*|n}^{1/2}\boldsymbol{\zeta}$. Whereas the former amounts to a standard solve, the latter often requires special considerations (Pleiss et al., 2020) and can be difficult to work with when typical square root decompositions prove impractical (Parker and Fox, 2012).

Lastly, we note that these techniques can be combined with inducing approximations for improved scaling in m and faster convergence of iterative solves. As a concrete example, consider the family of distributions $q(\mathbf{u}) = \mathcal{N}(\mathbf{u} \mid \boldsymbol{\mu}_u, \boldsymbol{\Sigma}_u)$ defined in terms of unconstrained means $\boldsymbol{\mu}_u \in \mathbb{R}^m$ and covariances $\boldsymbol{\Sigma}_u = (\mathbf{K}_{m,m}^{-1} + \boldsymbol{\Lambda})^{-1}$ parameterized by diagonal matrices $\boldsymbol{\Lambda} = \text{diag}(\boldsymbol{\lambda})$ with $\boldsymbol{\lambda} \in \mathbb{R}_+^m$. This family only consists of $2m$ free parameters, but is known to contain the optimal q when $\hat{\mathbf{y}}$ is Gaussian and $m \geq n$ (Seeger, 1999; Opper and Archambeau, 2009). Rewriting $\boldsymbol{\Sigma}_u$ using the Woodbury formula reveals that \mathbf{u} itself may be expressed as

$$\mathbf{u} \stackrel{\text{d}}{=} \mathbf{f}_m + \mathbf{K}_{m,m}(\mathbf{K}_{m,m} + \boldsymbol{\Lambda})^{-1}(\boldsymbol{\mu}_u - \mathbf{f}_m - \boldsymbol{\varepsilon}) \quad \boldsymbol{\varepsilon} \sim \mathcal{N}(\mathbf{0}, \boldsymbol{\Lambda}). \quad (28)$$

Combining this observation with (27) and simplifying gives the pathwise expression⁹

$$(f \mid \mathbf{u})(\cdot) \stackrel{\text{d}}{=} f(\cdot) + k(\cdot, \mathbf{Z})(\mathbf{K}_{m,m} + \boldsymbol{\Lambda})^{-1}(\boldsymbol{\mu}_u - \mathbf{f}_m - \boldsymbol{\varepsilon}). \quad (29)$$

This result closely resembles the Gaussian update (25), with $\boldsymbol{\mu}_u$ playing the role of \mathbf{y} and $\boldsymbol{\varepsilon}$ again acting as a (heteroskedastic) noise term. Owing to the appearance of $\boldsymbol{\Lambda}$ in the inverse however, the resulting linear system is substantially better-conditioned than that of naïve alternatives and can therefore be accurately solved in fewer iterations.

5.5 Finite-dimensional approximate posteriors

The Bayesian linear model $f^{(w)}(\cdot) = \boldsymbol{\phi}(\cdot)^\top \mathbf{w}$ introduced in Section 4 can be seen as the weight-space interpretation of a Gaussian processes (Rasmussen and Williams, 2006), whose covariance function may be explicitly written in terms of the finite-dimensional feature map $\boldsymbol{\phi} : \mathcal{X} \rightarrow \mathbb{R}^\ell$. Another option is therefore to perform a (Gaussian) pathwise update in terms of this finite-dimensional GP prior as

$$(f \mid \mathbf{y})(\cdot) \stackrel{\text{d}}{=} f(\cdot) + \boldsymbol{\phi}(\cdot)\boldsymbol{\Phi}_n^\top(\boldsymbol{\Phi}_n\boldsymbol{\Phi}_n^\top + \sigma_\varepsilon^2\mathbf{I})^{-1}(\mathbf{y} - \mathbf{f}_n - \boldsymbol{\varepsilon}), \quad (30)$$

9. This same line of reasoning leads to a *rank-1 pathwise update* for cases where conditions arrive online.

where $\Phi_n = \phi(\mathbf{X}_n)$ is an $n \times \ell$ feature matrix and $\varepsilon \sim \mathcal{N}(0, \sigma_\varepsilon^2 \mathbf{I})$ denotes measurement noise. Here, we have chosen to report the weight-space pathwise update for Gaussian likelihoods because $\Phi_n \Phi_n^\top$ is typically singular or otherwise sufficiently ill-conditioned for a Cholesky or similar decomposition to fail. Note that (30) implicitly updates the weights \mathbf{w} . Further, because we have used the basis induced by the feature map ϕ to represent both prior and update, the same result may be achieved by sampling generating a draw from the conditional distribution $p(\mathbf{w} \mid \mathbf{y})$. When ϕ consists of random Fourier features, this weight-space approximation delivers competitive performance for $\ell \geq n$. As n grows in relation to ℓ , however, this approximation begins to suffer from the variance starvation phenomenon discussed in Section 4.5.

Similar considerations apply when working with other methods for approximating GP posteriors in terms of finite-dimensional basis expansions. For example, if we construct a Gaussian process from m canonical basis functions $k(\cdot, \mathbf{Z})$ (Wahba, 1990; Smola and Bartlett, 2001), the resulting model typically reverts to deterministically predicting the prior mean away from locations \mathbf{Z} . This pathology occurs because we have decided to work solely in terms of the canonical basis functions, which are local for commonly used kernels. Previous works, such as (Rasmussen and Quinero-Candela, 2005), have proposed to *augment* $k(\cdot, \mathbf{Z})$ with one (or more) additional basis functions $k(\cdot, \mathbf{z})$, where $\mathbf{z} \in \mathcal{X}$ is typically chosen to lie in the vicinity of a test location \mathbf{x}_* . See Quinero-Candela et al. (2007) for extended discussion of these methods.

We may also think to employ a finite number of canonical basis functions in more sophisticated ways. For instance, we may define the m inducing locations \mathbf{Z} to lie on regularly spaced grid. As discussed in Section 4.1, this design choice endows $\mathbf{K}_{m,m} = k(\mathbf{Z}, \mathbf{Z})$ with special structure (circulant matrix) that we may exploit to dramatically reduce the cost of many standard matrix operations. We may now use kernel interpolation methods (Wilson and Nickisch, 2015) to build an approximate prior from this grid-based canonical basis $k(\cdot, \mathbf{Z})$. Pleiss et al. (2018) combine this approximate prior with techniques from the literature on iterative solvers to construct a low-rank location-scale transform (17) that affords linear time sampling. Provided that \mathbf{Z} is sufficiently dense in \mathbf{X} (so as to be reasonably close to the test locations), this method provides an alternative means of efficiently sampling from GP posteriors.

5.6 Discussion

By now, we have explored a variety of techniques for sampling from GP posteriors. We have tried to convey that, in our view, each of these methods is well-suited for a particular type of problem. To help build practical intuition for these niches, we conducted a simple, controlled experiment.

Here, our goal is to better understand how different methods balance the tradeoff of accuracy and cost. We measured accuracy in terms of 2-Wasserstein distances of empirical distributions from the true posterior and cost in terms of runtimes. To eliminate confounding variables, we assumed a known Matérn-5/2 prior on random functions $f : \mathbb{R}^4 \rightarrow \mathbb{R}$. Samples from said prior were drawn at 1024 test locations \mathbf{X}_* and n training locations \mathbf{X}_n , both chosen uniformly at random, using either location-scale transforms or random Fourier features. Given Gaussian observations \mathbf{y} , pathwise updates were then carried out in Gaussian, sparse,

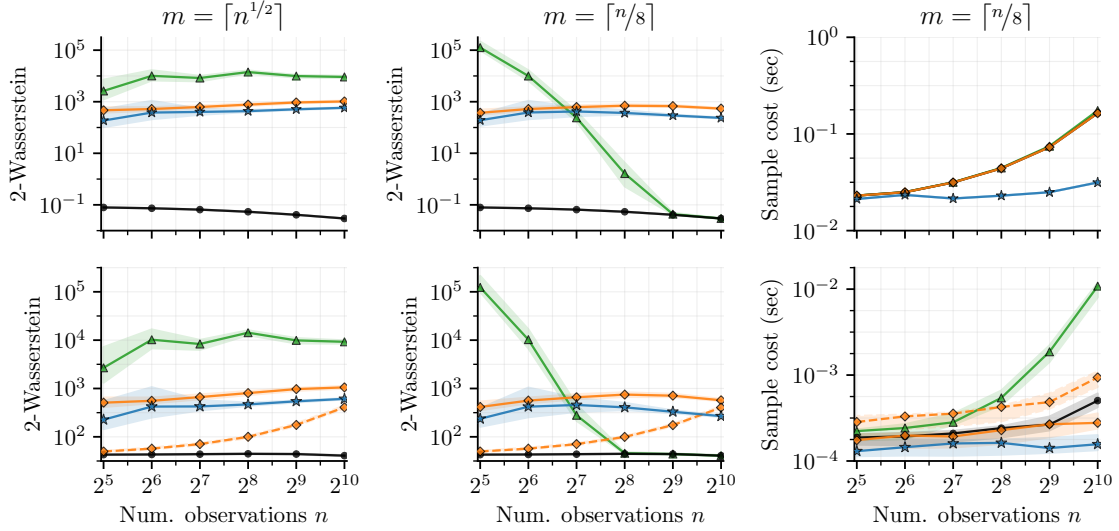


Figure 4: Accuracy and cost of different methods for sampling from GP posteriors given n observations: for details, see Section 5.6. Samples from the prior are generated using either location-scale (*top*) or $\ell = 4096$ random Fourier features (*bottom*). We denote Gaussian updates by black dots, sparse updates by blue stars, CG+ updates by green triangles, and RFF updates by orange diamonds. All results are reported as medians and interquartile ranges measured over 64 trials and asymptotic costs of sparse, CG+, and RFF updates were matched—save for on the bottom, where RFF is also shown (dashed orange) using the same $\ell + m$ features to represent both prior and update. *Left and middle*: 2-Wasserstein distances of empirical distributions of a million samples from the ground truth GP posterior. *Right*: Time taken to generate a sample of $(\mathbf{f}_* | \cdot) \in \mathbb{R}^{1024}$ without caching of terms related to \mathbf{X}_* .

and CG+ fashion. We used variational inference to learn sparse updates at m inducing locations \mathbf{Z} . For fair comparison, CG+ and its partial-pivoted-Cholesky-based preconditioner were each run for m iterations. Results are reported for two different schedules of m as a function of n .

Overall, we see that different methods perform well in different regimes. In all cases, approximating the prior using $\ell = 4096$ random Fourier features introduces a small amount of error, but significantly reduces the cost of sampling. Note that, when using RFF to represent the prior, the only remaining linear systems (those of the pathwise updates) can be efficiently solved by reusing the Cholesky factor of $\mathbf{K}_{n,n} + \sigma^2 \mathbf{I}$. As expected, the true Gaussian update produces the highest quality samples, albeit at the (asymptotically) greatest expense. Sparse updates substantially reduce these overheads in exchange for introducing a non-trivial, but consistent, loss in accuracy. Consistent with the analysis in Section 5.5, the RFF update perform admirably when the number of features employed is much greater than n .

Depending on the choice of m relative to n , conjugate-gradient-based updates may introduce either a negligible or an exorbitant amount error. This contrast is explained for by the fact that, in practice, one typically runs CG until it has converged within a tolerated

degree of error (rather than for a fixed number of steps). More generally, iterative solvers shine in cases where n (or m) is in excess of a few thousand, by allowing us to perform updates subject to many more conditions.

These empirical results help to characterize the behaviors of errors introduced by different approximation schemes, but leave many questions unanswered. In order to fill in some of the remaining gaps, we now analyze various types of approximation error in details.

6. Error analysis

Throughout this section, we assume that \mathcal{X} is a compact subset of an ambient space \mathcal{M} and proceed to analyze how errors introduced by different approximations to the pathwise representation of Gaussian process posteriors manifest on \mathcal{X} . By way of example, \mathcal{X} may be the n -dimensional unit hypercube $[0, 1]^d$ living inside of $\mathcal{M} = \mathbb{R}^d$. Further, we assume that training locations \mathbf{X}_n fill the space \mathcal{X} as $n \rightarrow \infty$.

In order to speak about this error, we require a suitable notion of distance on the space of probability distributions. We focus on 2-Wasserstein distances between Gaussian processes and supremum distance between covariances functions. Both of these metrics are guaranteed to be finite in most cases and thereby facilitate sensible comparison. Moreover, 2-Wasserstein distances majorize 1-Wasserstein distances, which (by Kantorovich–Rubinstein duality) control expectations of Lipschitz functionals—whereupon, they act as natural performance metrics for comparing Monte Carlo estimates based on samples from different distributions.

6.1 Posterior approximation error

We begin by adapting the results of Wilson et al. (2020) to the specific case of the approximate posterior $f^{(p)}$ formed by applying a canonical update (15) to a finite basis function prior $f^{(w)}$. We return to full results, which compare posteriors when applying Gaussian and sparse updates to RFF priors, in Section 6.3.

Proposition 5 *Assume that $\mathcal{X} \subseteq \mathbb{R}^d$ is compact and that the stationary kernel k is sufficiently regular for $f \sim \mathcal{GP}(\mu, k)$ to be almost surely continuous. Accordingly, if we define $C^{(1)} = \sqrt{2} \text{diam}(\mathcal{X})^{d/2} (1 + \|k\|_{C(\mathcal{X}^2)}^2 \|\mathbf{K}_{n,n}^{-1}\|_{L(\ell^\infty; \ell^1)}^2)^{1/2}$, then we have*

$$W_{2, L^2(\mathcal{X})}(f^{(p)}, f \mid \mathbf{y}) \leq C^{(1)} W_{2, C(\mathcal{X})}(f^{(w)}, f), \quad (31)$$

where $W_{2, L^2(\mathcal{X})}$ and $W_{2, C(\mathcal{X})}$ are the 2-Wasserstein distances over the Lebesgue space $L^2(\mathcal{X})$ and the space of continuous functions $C(\mathcal{X})$ equipped with the supremum norm, respectively, and where $\|\cdot\|_{C(\mathcal{X}^2)}$ denotes the supremum norm over continuous functions and $\|\cdot\|_{L(\ell^\infty; \ell^1)}$ denotes the operator norm between ℓ^∞ and ℓ^1 spaces.

Proof Wilson et al. (2020), Proposition 3. ■

Proposition 6 *Under the same assumptions, let $k^{(f|\mathbf{y})}$, $k^{(w)}$, $k^{(p)}$ denote the respective covariance functions of $f \mid \mathbf{y}$, $f^{(w)}$, $f^{(p)}$ and let $C^{(2)} = n(1 + \|\mathbf{K}_{n,n}^{-1}\|_{C(\mathcal{X}^2)} \|k\|_{C(\mathcal{X}^2)})^2$. Then*

$$\mathbb{E}_\phi \|k^{(p)} - k^{(f|\mathbf{y})}\|_{C(\mathcal{X}^2)} \leq C^{(2)} \|k^{(w)} - k\|_{C(\mathcal{X}^2)}. \quad (32)$$

Moreover, when $f^{(w)}$ is a random Fourier feature approximation of the prior, it follows that

$$\mathbb{E}_\phi \|k^{(p)} - k^{(f|\mathbf{y})}\|_{C(\mathcal{X}^2)} \leq \ell^{-1/2} C^{(2)} C^{(3)}, \quad (33)$$

where $C^{(3)}$ is one of several possible constants given by Sutherland and Schneider (2015).

Proof Wilson et al. (2020), Proposition 4. ■

Together, propositions 5 and 6 show that error in the approximate prior $f^{(w)}$ controls the error in the resulting approximate posterior $f^{(p)}$. Note that these bounds are not tight, as constants $C^{(1)}$ and $C^{(2)}$ both depend on the number of observations n . Based on this observation, it is tempting to think that the error in $f^{(p)}$ therefore increases in n . Empirically, however, the opposite trend is observed: the error in $f^{(p)}$ actually diminishes in n , see Figure 3 of Wilson et al. (2020). To better understand this behavior, we now study the conditions under which a pathwise update may counteract the error introduced by an approximate prior.

6.2 Contraction of approximate posteriors with noise-free observations

This section formalizes the following syllogism: (i) posterior $f | \mathbf{y}$ and approximate posterior $f^{(p)}$ have the same mean, (ii) as n increases, both posteriors contract to their means, (iii) therefore, as n increases, the error introduced by the approximate prior $f^{(w)}$ washes out.

To begin, let $\phi : \mathcal{M} \rightarrow \mathbb{R}^\ell$ be an ℓ -dimensional feature map on ambient space \mathcal{M} consisting of linearly independent basis functions ϕ_i , in the following sense. We will say that $f^{(w)}$ is a *standard normal Bayesian linear model* if it admits the representation

$$f^{(w)}(\cdot) = \sum_{i=1}^{\ell} w_i \phi_i(\cdot) \quad w_i \sim \mathcal{N}(0, 1). \quad (34)$$

This description includes the Fourier feature and Karhunen–Loève approximations described in Section 4. As additional notation, let $\Phi_n = \phi(\mathbf{X}_n)$ be an $n \times \ell$ matrix of features and \mathcal{H}_k be the reproducing kernel Hilbert space of k . We say that a function ϕ *lies locally* in \mathcal{H}_k for a compact $\mathcal{X} \subseteq \mathcal{M}$ when there exists a function $\psi \in \mathcal{H}_k$ that agrees with ϕ on \mathcal{X} , i.e., $\phi|_{\mathcal{X}} = \psi|_{\mathcal{X}}$.

For kernels with known reproducing kernel Hilbert spaces, assessing whether or not ϕ_i lies locally in \mathcal{H}_k is often straightforward. For example, the RKHS of a Matérn- $\nu/2$ kernel is the Sobolev space of order $\nu + d/2$. For integer values of $\nu + d/2$, this is the space of square-integrable functions with $\nu + d/2$ square-integrable derivatives. Random Fourier features $\phi_i(\mathbf{x}) = \cos(\omega_i^\top \mathbf{x} + \tau_i)$ readily satisfy this requirement: we may *mollify* ϕ_i such that these basis functions (and their derivatives) are square-integrable by simply multiplying them by an infinitely-differentiable function that ensures they decay to zero outside of \mathcal{X} . Furthermore, when \mathcal{M} is a compact metric space, the truncated Karhunen–Loève approximations to the prior trivially satisfies this condition, since eigenfunctions ϕ_i belong to \mathcal{H}_k by construction. We are now ready to state and prove the main claim.

Proposition 7 Suppose $\mathcal{X} \subseteq \mathcal{M}$ is compact and that each of the ℓ basis functions ϕ_i used to construct the standard normal Bayesian linear model $f^{(w)}$ lies locally in \mathcal{H}_k . If the points $\mathbf{X}_n \subseteq \mathcal{X}$ used to condition the approximate posterior $f^{(p)}$ are such that $f \mid \mathbf{y}$ satisfies $\sup_{\mathbf{x} \in \mathcal{X}} k^{(f|\mathbf{y})}(\mathbf{x}, \mathbf{x}) \leq \varepsilon$, then it follows that

$$\sup_{\mathbf{x} \in \mathcal{X}} |k^{(p)}(\mathbf{x}, \mathbf{x})| \leq C^{(4)} \varepsilon \quad (35)$$

where we have defined $C^{(4)} = \ell \max_i \inf \left\{ \|\psi_i\|_{\mathcal{H}_k}^2 : \psi_i|_{\mathcal{X}} = \phi_i|_{\mathcal{X}}, \psi_i \in \mathcal{H}_k \right\}$.

Proof Write

$$\begin{aligned} f^{(p)}(\cdot) &= \phi(\cdot)^\top \mathbf{w} - k(\cdot, \mathbf{X}_n) \mathbf{K}_{n,n}^{-1} (\mathbf{y} - \Phi_n \mathbf{w}) \\ &= \underbrace{\left(\phi(\cdot)^\top - k(\cdot, \mathbf{X}_n) \mathbf{K}_{n,n}^{-1} \Phi_n \right)}_{\text{controls variance}} \mathbf{w} + \underbrace{k(\cdot, \mathbf{X}_n) \mathbf{K}_{n,n}^{-1} \mathbf{y}}_{\text{deterministic}} \end{aligned} \quad (36)$$

and

$$\begin{aligned} \text{Var}(f^{(p)}(\cdot)) &= \mathbb{E} \left| \left(\phi(\cdot)^\top - k(\cdot, \mathbf{X}_n) \mathbf{K}_{n,n}^{-1} \Phi_n^\top \right) \mathbf{w} \right|^2 \\ &\leq \ell \max_i \left| \phi_i(\cdot) - k(\cdot, \mathbf{X}_n) \mathbf{K}_{n,n}^{-1} \phi_i(\mathbf{X}_n) \right|^2 \end{aligned} \quad (37)$$

where, on the right, we have used the fact that $\mathbb{E} \|\mathbf{w}\|^2 = \ell$. By the dual representation of the RKHS norm, we now have

$$\begin{aligned} \left| \phi_i(\mathbf{x}_*) - \mathbf{K}_{*,n} \mathbf{K}_{n,n}^{-1} \phi_i(\mathbf{X}_n) \right| &\leq \|\phi_i\|_{\mathcal{H}_k} \sup_{g \in \mathcal{H}_k : \|g\|_{\mathcal{H}_k} = 1} |g(\mathbf{x}_*) - \mathbf{K}_{*,n} \mathbf{K}_{n,n}^{-1} g(\mathbf{X}_n)| \\ &= \|\phi_i\|_{\mathcal{H}_k} \left\| k(\cdot, \mathbf{x}_*) - k(\cdot, \mathbf{X}_n) \mathbf{K}_{n,n}^{-1} \mathbf{K}_{n,*} \right\|_{\mathcal{H}_k} \\ &= \|\phi_i\|_{\mathcal{H}_k} \underbrace{\sqrt{k(\mathbf{x}_*, \mathbf{x}_*) - \mathbf{K}_{*,n} \mathbf{K}_{n,n}^{-1} \mathbf{K}_{n,*}}}_{\text{denote by } \mathcal{P}_{\mathbf{X}}(\mathbf{x}_*)} \end{aligned} \quad (38)$$

where, because ϕ_i lies locally in \mathcal{H}_k , we may replace it with any $\psi_i \in \mathcal{H}_k : \psi_i|_{\mathcal{X}} = \phi_i|_{\mathcal{X}}$. Noting that $\mathcal{P}_{\mathbf{X}}(\cdot) = \sqrt{k^{(f|\mathbf{y})}(\cdot, \cdot)}$ and collecting these terms together gives the result. \blacksquare

This proposition shows that the approximate posterior $f^{(p)}$ contracts at the same rate as the true posterior $f \mid \mathbf{y}$. Consequently, both posteriors contract to the same mean as n increases and the error in $f^{(p)}$ vanishes. More formally, we have the following.

Corollary 8 Under the previous set of assumptions, as $\sup_{\mathbf{x} \in \mathcal{X}} k^{(f|\mathbf{y})}(\mathbf{x}, \mathbf{x}) \rightarrow 0$, we have

$$\sup_{\mathbf{x}, \mathbf{x}' \in \mathcal{X}} |k^{(p)}(\mathbf{x}, \mathbf{x}') - k^{(f|\mathbf{y})}(\mathbf{x}, \mathbf{x}')| \rightarrow 0. \quad (39)$$

Proof Begin by apply the triangle inequality to the above and, subsequently, use the Cauchy-Schwartz inequality to bound $k(\mathbf{x}, \mathbf{x}') \leq \sqrt{k(\mathbf{x}, \mathbf{x})} \sqrt{k(\mathbf{x}', \mathbf{x}')}$, i.e.,

$$\begin{aligned} \sup_{\mathbf{x}, \mathbf{x}' \in \mathcal{X}} |k^{(p)}(\mathbf{x}, \mathbf{x}') - k^{(f|\mathbf{y})}(\mathbf{x}, \mathbf{x}')| &\leq \sup_{\mathbf{x}, \mathbf{x}' \in \mathcal{X}} |k^{(p)}(\mathbf{x}, \mathbf{x}')| + \sup_{\mathbf{x}, \mathbf{y} \in \mathcal{X}} |k^{(f|\mathbf{y})}(\mathbf{x}, \mathbf{x}')| \\ &\leq \sup_{\mathbf{x} \in \mathcal{X}} |k^{(p)}(\mathbf{x}, \mathbf{x})| + \sup_{\mathbf{x} \in \mathcal{X}} |k^{(f|\mathbf{y})}(\mathbf{x}, \mathbf{x})|. \end{aligned} \quad (40)$$

In the final expression, convergence of the former term is given by Proposition 7 while the latter goes to zero by assumption. \blacksquare

The analogous result for Wasserstein distances between $f \mid \mathbf{y}$ and $f^{(p)}$ immediately follows.

Corollary 9 *Under the previous set of assumptions, as $\sup_{\mathbf{x} \in \mathcal{X}} k^{(f|\mathbf{y})}(\mathbf{x}, \mathbf{x}) \rightarrow 0$, we have*

$$W_{2,L^2(\mathcal{X})}(f \mid \mathbf{y}, f^{(p)}) \rightarrow 0. \quad (41)$$

Proof Since $L^2(\mathcal{X})$ is a norm and $\mathbb{E}(f \mid \mathbf{y}) = \mathbb{E}(f^{(p)})$, it follows that

$$W_{2,L^2(\mathcal{X})}(f \mid \mathbf{y}, f^{(p)}) = W_{2,L^2(\mathcal{X})} \left(\underbrace{f(\cdot) - k(\cdot, \mathbf{X}_n) \mathbf{K}_{n,n}^{-1} f(\mathbf{X}_n)}_{f_0 \mid \mathbf{y}}, \underbrace{\phi(\cdot)^\top \mathbf{w} - k(\cdot, \mathbf{X}_n) \mathbf{K}_{n,n}^{-1} \Phi_n \mathbf{w}}_{f_0^{(p)}} \right) \quad (42)$$

where both terms have mean zero. Let \emptyset be an almost surely zero stochastic process over \mathcal{X} . Then, by the triangle inequality,

$$W_{2,L^2(\mathcal{X})}(f_0 \mid \mathbf{y}, f_0^{(p)}) \leq W_{2,L^2(\mathcal{X})}(f_0 \mid \mathbf{y}, \emptyset) + W_{2,L^2(\mathcal{X})}(\emptyset, f_0^{(p)}). \quad (43)$$

Expanding the definition of Wasserstein distances $W_{2,L^2(\mathcal{X})}$ before using Tonelli's theorem to change the order of integration gives

$$\begin{aligned} W_{2,L^2(\mathcal{X})}(f_0 \mid \mathbf{y}, f_0^{(p)}) &\leq \left(\mathbb{E} \| (f_0 \mid \mathbf{y}) - \emptyset \|_{L^2(\mathcal{X})}^2 \right)^{1/2} + \left(\mathbb{E} \| \emptyset - f_0^{(p)} \|_{L^2(\mathcal{X})}^2 \right)^{1/2} \\ &= \left(\int_{\mathcal{X}} k^{(f|\mathbf{y})}(\mathbf{x}, \mathbf{x}) d\mathbf{x} \right)^{1/2} + \left(\int_{\mathcal{X}} k^{(p)}(\mathbf{x}, \mathbf{x}) d\mathbf{x} \right)^{1/2}, \end{aligned} \quad (44)$$

where both terms in the final expression converge to zero by compactness of \mathcal{X} together with Proposition 7. \blacksquare

Together, these claims demonstrate that the approximate posterior $f^{(p)}$ formed by applying the canonical update (15) to a suitably chosen approximate prior $f^{(w)}$ *inherits* the contractive properties of the true posterior $f \mid \mathbf{y}$.

Here, a simple counterexample helps clarify the notion of a “suitable” approximate prior. Consider the approximation formed by redefining $f^{(w)}$ to be a GP prior with the Kronecker delta kernel $c(\mathbf{x}, \mathbf{x}') = \mathbb{1}_{\mathbf{x}=\mathbf{x}'}$. For any location $\mathbf{x} \in \mathcal{X} \setminus \mathbf{X}_n$, the variance of the approximate posterior $f^{(p)}$ is given by

$$k^{(p)}(\mathbf{x}, \mathbf{x}) = c(\mathbf{x}, \mathbf{x}) + k(\mathbf{x}, \mathbf{X}_n) \mathbf{K}_{n,n}^{-1} \mathbf{C}_{n,n} \mathbf{K}_{n,n}^{-1} k(\mathbf{X}_n, \mathbf{x}) = 1 + k(\mathbf{x}, \mathbf{X}_n) \mathbf{K}_{n,n}^{-2} k(\mathbf{X}_n, \mathbf{x}), \quad (45)$$

where we have dropped the $-2c(\mathbf{x}, \mathbf{X}_n) \mathbf{K}_{n,n}^{-1} k(\mathbf{X}_n, \mathbf{x}) = \mathbf{0}$ term from the above calculation. Since the second of the two term on the right is guaranteed non-negative, $k^{(p)}(\mathbf{x}, \mathbf{x})$ is bounded from below by 1. For this choice of approximate prior, the posterior variance and, hence, the approximation error of $f^{(p)}$ does not contract as n increases.

Assuming that $f^{(w)}$ is a standard normal Bayesian linear model with basis functions lying locally in \mathcal{H}_k suffices to avoid this issue. More generally, an analogous inequality (albeit with a different constant) can be obtained via the same line of reasoning without placing an i.i.d. assumption on the weights of $f^{(w)}$. As a potential point of interest for some readers, we note that contraction of the true posterior is well-studied, with strong ties to the kernel interpolation literature. Kanagawa et al. (2018) reviews these connections in greater detail. In particular, Theorem 5.4 of said work shows how the *power function* $\mathcal{P}_{\mathbf{X}}$ can be bounded in terms of the *local fill distance*, which governs the proximity of locations \mathbf{X}_n as n increases.

6.3 Sparse approximations and Gaussian observations

We now examine the error introduced by using the sparse pathwise update (27) to construct approximate posteriors. As notation, we write $f^{(s)}$ and $f^{(d)}$ for the approximate posteriors formed by applying the sparse update to the true prior f and to the approximate prior $f^{(w)}$, respectively. Results discussed here mirror those presented in Wilson et al. (2020). Appealing to the triangle inequality, we have

$$\begin{aligned} W_{2,L^2(\mathcal{X})}(f^{(d)}, f \mid \mathbf{y}) &\leq \underbrace{W_{2,L^2(\mathcal{X})}(f^{(d)}, f^{(s)})}_{\text{error in approximate prior}} + \underbrace{W_{2,L^2(\mathcal{X})}(f^{(s)}, f \mid \mathbf{y})}_{\text{error in sparse update}} \\ \mathbb{E}_\phi \|k^{(d)} - k^{(f|\mathbf{y})}\|_{C(\mathcal{X}^2)} &\leq \underbrace{\mathbb{E}_\phi \|k^{(d)} - k^{(s)}\|_{C(\mathcal{X}^2)}}_{\text{error in approximate prior}} + \underbrace{\|k^{(s)} - k^{(f|\mathbf{y})}\|_{C(\mathcal{X}^2)}}_{\text{error in sparse update}}. \end{aligned} \quad (46)$$

From here, any of the previously presented propositions enable us to control the total error. For the first terms on the right, the same arguments as before lead to the same results, however, the involved constants will change, since the sparse update now assumes the role of the canonical one. The latter terms do not involve approximations to the prior and, therefore, may be analyzed in isolation. Note that a similar statement holds for the Gaussian pathwise update (25).

As a final remark, we note that the total error (46) may be reduced by augmenting the sparse update with an additional basis function $k(\cdot, \mathbf{z})$ (see Section 5.5). For clarity, we note that this process involves augmenting the inducing distribution $q(\mathbf{u})$ without altering $f^{(d)}$, which may be done analytically. Following Section 6.2, the variance (and hence the error) of $f^{(d)}$ when conditioning on (rather than marginalizing over) \mathbf{u} diminishes as m increases. The variance of $f^{(d)}$ does not change however, it is simply absorbed by the kernel basis functions $k(\cdot, \mathbf{Z})$.

7. Applications

This section examines the practical consequences of pathwise conditioning in terms of a curated set of representative tasks. Throughout, we focus on how pathwise methods for efficiently generating function draws from GP posteriors enable us to overcome common obstacles and open doors for new research.

7.1 Optimizing black-box functions

Global optimization pertains to the challenge of efficiently identifying a global minimizer

$$\mathbf{x}_* \in \mathbf{X}_* = \arg \min_{\mathbf{x} \in \mathcal{X}} f(\mathbf{x}) \quad (47)$$

of a black-box function $f : \mathcal{X} \rightarrow \mathbb{R}$. Since f is a black-box, our understanding of its behavior is limited to a set of (noisy) observations \mathbf{y} at locations \mathbf{X}_n . Gaussian processes are a natural and widely used way of representing possible functions $f \mid \mathbf{y}$ (Moćkus, 1975; Srinivas et al., 2009; Frazier, 2018). In these cases, we therefore reason about global minimizers (47) in terms of a belief over the random set

$$\mathbf{X}_*^{(f|\mathbf{y})} = \arg \min_{\mathbf{x} \in \mathcal{X}} (f \mid \mathbf{y})(\mathbf{x}). \quad (48)$$

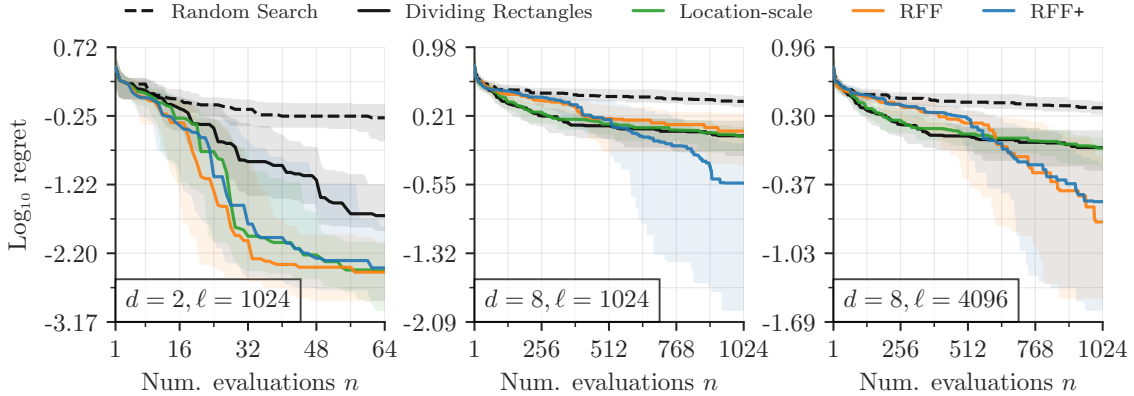


Figure 5: Median performances and interquartile ranges of TS methods and popular baselines when optimizing d -dimensional functions drawn from known GP priors. Location-scale TS perform well in low-dimensional settings (left), but struggles as d increase due to its inability to efficiently utilize gradient information. RFF posteriors enable us to generate function draws, but many more basis functions $b = \ell + n$ than data points n (middle vs. right). Gaussian updates of draws from RFF priors (RFF+) avoids these pitfalls and consistently matches or outperforms competing strategies.

Approaches to these problems are often characterized as striking a balance between two competing agendas: the need to learn about f 's global behavior by exploring the domain \mathcal{X} and the need to obtain (potentially local) minimizers by exploiting what is already known.

Thompson sampling (TS) is a classic decision-making strategy that balances the tradeoff between exploration and exploitation by sampling actions $\mathbf{x} \in \mathcal{X}$ in proportion to the probability that $\mathbf{x} \in \mathbf{X}_*^{(f|\mathbf{y})}$ (Thompson, 1933). At first glance, this task may seem daunting, since $\mathbf{X}_*^{(f|\mathbf{y})}$ is random. For any given draw of $f | \mathbf{y}$, however, $\mathbf{X}_*^{(f|\mathbf{y})}$ is deterministic. Accordingly, we may Thompson sample an action by drawing a function $f | \mathbf{y}$ and, subsequently, finding a pathwise global minimizer. Thompson sampling's relative simplicity makes it a natural test bed for evaluating different sampling strategies, while its real-world performance (Chapelle and Li, 2011) assures its ongoing relevance in applied settings.

One of Thompson sampling's key strengths is its ability to gracefully accommodate simultaneous evaluation of $\kappa > 1$ designs (Hernández-Lobato et al., 2017; Kandasamy et al., 2018). While many GP-based search strategies admit parallel variants (Snoek et al., 2012; Wilson et al., 2020), they typically scale poorly in κ . In our experiments, we employ TS in parallel synchronous fashion by concurrently evaluating a pathwise minimizer from each of $\kappa = d$ independently generated draws of $f | \mathbf{y}$. Note, however, that this choice was not found to significantly influence our results.

An excerpt of our results is shown in Figure 5. For full details regarding the design of these experiments, implementation of TS, and extended results, see Wilson et al. (2020). In short, we experimented in a controlled setting where black-box functions were drawn from known GP priors. Here, we discuss the performance of TS under three different sampling strategies: (i) location-scale sampling from the posterior, (ii) RFF-based sampling from

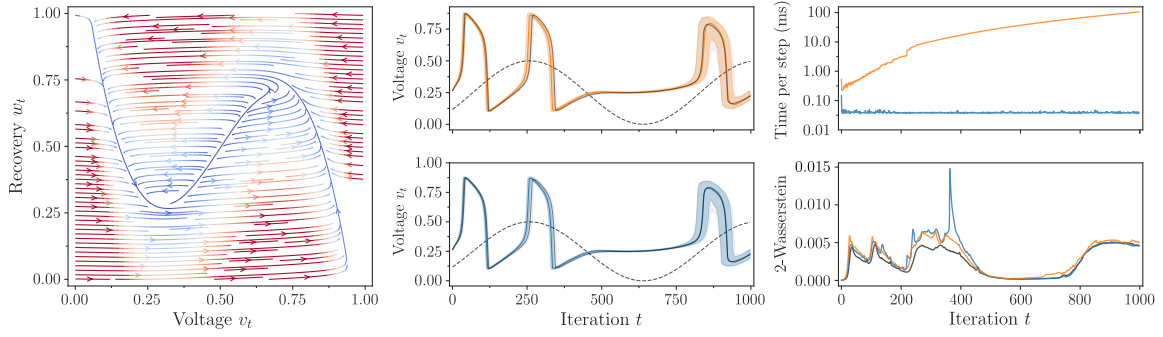


Figure 6: Simulation of a noisy FitzHugh-Nagumo model neuron using a sparse GP. *Left*: Phase portrait of the true drift function subject to a current injection $u(t) = 0.5$. *Top middle*: Summary (medians and interquartile ranges) of 1000 voltage traces in response to a sinusoidal current (dashed line) generated using a sequence of location-scale transforms, *Bottom middle*: Summary of 1000 voltage traces using drift functions drawn by applying a sparse update to a random Fourier prior. *Top right*: Comparison of simulation runtimes. *Bottom right*: Sinkhorn estimates (Cuturi, 2013) to 2-Wasserstein distances of model-based and ground truth state distributions at each step. The noise floor (gray) was found using additional ground truth simulations.

the posterior (iii) RFF-based sampling from the prior with Gaussian pathwise updates (25). Key trends are as follows. First, location-scale methods’ inability to use gradient information to efficiently find pathwise minimizers causes its performance to wane as the dimensionality of the search space d increases. Second, RFF struggles to represent the posterior when the allocated number of basis functions $b = \ell + n$ is not sufficiently larger than the number of observations n . Lastly, decoupling the representation of the prior and data—by using canonical basis functions $k(\cdot, \mathbf{X}_n)$ to define a pathwise update of draws from a RFF prior—allows us to reliably generate pathwise-differentiable functions $f \mid \mathbf{y}$.

7.2 Simulating dynamical systems

Gaussian process posteriors are commonly used to simulate complex, real-world phenomena in cases where we are unable to actively collecting additional data. These phenomena frequently amount to dynamical systems that describe how states evolve over time. For example, state-of-the-art methods for autonomous control of robotics system rely on GP-based forecasting to efficiently solve for underlying reinforcement learning problems (Deisenroth and Rasmussen, 2011; Kamthe and Deisenroth, 2018).

In this example, we place a Gaussian process prior on the *drift* $f : \mathcal{X} \times \mathcal{U} \rightarrow \mathcal{X}$ of a time-invariant system as a function of a state vector $\mathbf{x}_t \in \mathcal{X}$ and control signal $\mathbf{u}_t \in \mathcal{U}$ at time t . Under a Euler-Maruyama discretization scheme with increments Δt , the corresponding stochastic differential equation (SDE) is given as

$$\Delta \mathbf{x}_t = \mathbf{x}_{t+1} - \mathbf{x}_t = f(\mathbf{x}_t, \mathbf{u}_t) \Delta t + \sqrt{\Delta t} \boldsymbol{\varepsilon} \quad \boldsymbol{\varepsilon} \sim \mathcal{N}(\mathbf{0}, \boldsymbol{\Sigma}_{\boldsymbol{\varepsilon}}), \quad (49)$$

where $\boldsymbol{\varepsilon}$ represents process *diffusion*. Given n observations of the form $\mathbf{y}_t = \mathbf{x}_{t+\tau} - \mathbf{x}_t$, we are interested in generating drift functions $f \mid \mathbf{Y}$ in order to simulate possible state trajectories

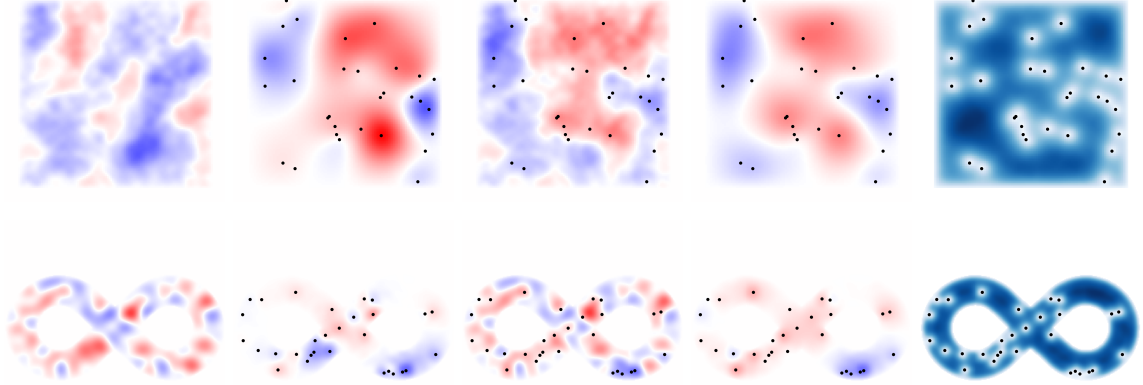


Figure 7: Examples of samples from Matérn prior conditioned to have zero on the boundary of the domain. Columns demonstrate (from leftmost to rightmost): a prior sample, an update, a posterior sample, empirical posterior mean over 1024 samples, empirical standard deviation over 1024 samples. Top row illustrates a rectangular domain where the Laplacian eigenpairs are available in the closed form. Bottom row demonstrates the samples on a non-trivial domain where the eigenpairs are approximated numerically.

$\mathbf{x}_{1:T} = (\mathbf{x}_1, \dots, \mathbf{x}_T)$ subject to an initial condition \mathbf{x}_0 and a control function $u : \mathcal{X} \rightarrow \mathcal{U}$ such that $\mathbf{u}_t = u(\mathbf{x}_t)$. We then use these trajectories to identify a function u that optimizes some objective.

Following Section 4.1, location-scale methods are poorly suited for the task of *unrolling* $\mathbf{x}_{1:*}$, since accounting for the previous sample of $f(\mathbf{x}_{t-\tau}, \mathbf{u}_{t-\tau})$ require us to iteratively recondition f at each step. Whereas this approach to unrolling scales cubically in T , pathwise approaches based on simulating function $f \mid \mathbf{y}$ scale linearly. To heighten this contrast, we trained a sparse GP to represent a classical model of a biological neural (FitzHugh, 1961; Nagumo et al., 1962), shown in Figure 6. While both sampling strategies accurately portray this SDE, the dramatic price differential between these methods is such that the former ran in 10 hours while the latter ran in 20 seconds.

7.3 Conditioning boundary-constrained Gaussian processes

Here, we illustrate how to use the ideas described in the preceding sections to perform efficient posterior sampling for Matérn Gaussian processes with imposed boundary conditions. This mirrors the situation studied by Solin and Kok (2019).

Whittle (1963) proves that a Matérn GP f defined over \mathbb{R}^d satisfies the stochastic partial differential equation

$$\left(\frac{2\nu}{\kappa^2} - \Delta \right)^{\frac{\nu}{2} + \frac{d}{4}} f = \mathcal{W} \quad (50)$$

where \mathcal{W} is a (rescaled) white noise process, and Δ is the Laplacian. Following Solin and Kok (2019) and Rue and Held (2005), we restrict (50) onto a (well-behaved) compact domain $\mathcal{X} \subset \mathbb{R}^d$ and imposing Dirichlet boundary conditions $f|_{\partial\mathcal{X}} = 0$ to define a boundary-

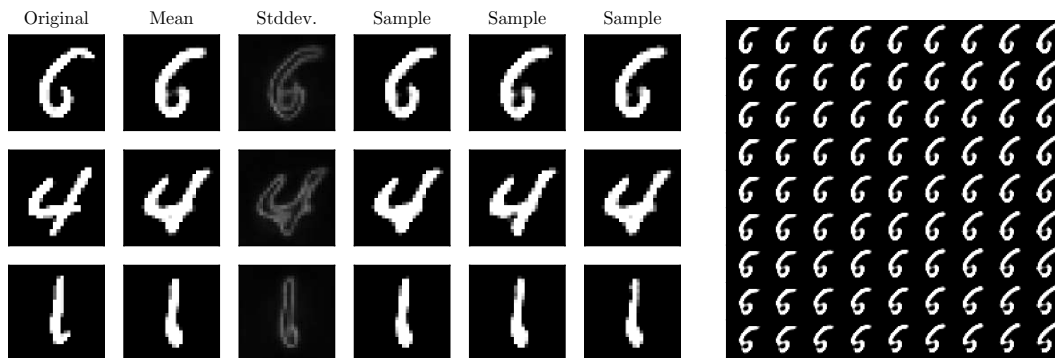


Figure 8: Reconstructions of MNIST digits by a deep convolutional GP trained to act as an autoencoder. *Left:* Mean and standard deviations of the (non-Gaussian) distribution over the reconstructions of randomly chosen test images are shown alongside three independently generated samples. *Right:* A 2-dimensional projection of a 25-dimensional latent space is found by performing SVD on the Jacobian of the mean response of the first decoder layer given an encoding of first image shown on the left. Reconstructions using the mean of each decoder layer are shown for a local walk in this 2-dimensional projected space.

constrained Matérn Gaussian process over \mathcal{X} . Solin and Kok (2019) demonstrate that such a prior admits the Karhunen–Loève expansion

$$f(\cdot) = \sum_{i=1}^{\infty} w_i \phi_i(\cdot) \quad w_i \sim \mathcal{N}\left(0, \frac{\sigma^2}{C_\nu} \left(\frac{2\nu}{\kappa^2} + \lambda_i\right)^{-\nu - \frac{d}{2}}\right) \quad (51)$$

where ϕ_i are eigenfunctions of the *boundary-constrained* Laplacian. We truncate this expansion to obtain the ℓ -dimensional Bayesian linear model $f^{(w)}$.

Figure 7 visualizes function draws from boundary-constrained priors and posterior for two choices of boundaries on \mathbb{R}^2 : namely, a rectangle and an infinity symbol. Note that eigenfunctions for rectangular regions of Euclidean domains are available analytically, while those of the infinity symbol are obtained numerically by solving a Helmholtz equation. Examining this figure, we see that the sample paths respect the Dirichlet boundary condition $f|_{\partial\mathcal{X}} = 0$. Karhunen–Loève expansions enables boundary-constrained GPs, which form an important class of non-stationary priors, to be used within the pathwise conditioning framework.

7.4 Evaluating deep Gaussian processes

When applying Gaussian process methods to novel problems, we are often faced with a natural dilemma: many phenomena of interest are definitively non-Gaussian. Since linear transformations of Gaussian random variables are Gaussian, we must look to nonlinear alternatives in order to represent these non-Gaussian phenomena. Since Gaussian random variables pushed forward through nonlinear functions seldom adhere to computationally convenient distributions, we are forced to trade tractability for expressivity.

This issue has recently come to the fore in the context of deep Gaussian processes (Damianou and Lawrence, 2013), which represent function priors as compositions

$$f(\cdot) = (f_T \circ f_{T-1} \circ \dots \circ f_1)(\cdot), \quad (52)$$

where $f_t \sim \mathcal{GP}(\mu_t, k_t)$ for $t = 1, \dots, T$. Following Salimbeni and Deisenroth (2017), sampling-based methods have become the standard approach for evaluating and training these models. Assuming (i) independent layers consisting of (ii) independent scalar-valued GPs (or linear combinations thereof), (52) can be efficiently evaluated without resorting to expensive matrix operations. When these assumptions are violated however, sampling-based evaluations of deep GPs may incur exorbitant costs. One such example was touched on in the previous section, where a deep GP is treated as a stochastic differential equation (Hegde et al., 2018). In these cases, placing a GP prior on the drift function results in non-trivial dependencies between “layers” $f(t, \cdot)$ and $f(t', \cdot)$.

Similar issues arise when sampling from (compositions of) multioutput GPs (van der Wilk et al., 2020). The remainder of this section focuses on one such case, namely deep convolutional GPs (Blomqvist et al., 2019; Dutordoir et al., 2020). Here, the overarching model is defined in close analogy to convolutional neural networks (van der Wilk et al., 2017): each layer consists of a set of independent maps that are convolved over local subsets (patches) of an image $\mathbf{x}_t \in \mathbb{R}^{h_t \times w_t \times c_t}$. For a convolutional neural network these *patch response functions* are affine transformations followed by some nonlinearity, for a convolutional Gaussian process they are draws from GP priors.

Since each of the c_t independent patch response functions produces $h_t \times w_t$ output features, the covariance of the Gaussian random variables $\mathbf{x}_t = f_t * \mathbf{x}_{t-1}$ is a block diagonal square matrix of order $c_t \times h_t \times w_t$. The cost for computing an associated matrix square root is therefore $\mathcal{O}(c_t \times h_t^3 \times w_t^3)$.¹⁰ By virtue of operating in terms of function draws, pathwise conditioning cleanly avoids this issue.

As an illustrative example, we trained a deep GP to act as an autoencoder for the MNIST dataset (LeCun and Cortes, 2010). As an encoder, we employ a sequence of three convolutional layers with 384 inducing patches $\mathbf{Z} \in \mathbb{R}^{3 \times 3 \times c_{t-1}}$ shared between $\{32, 32, 1\}$ convolutional GPs. Strides and padding are chosen to produce a 25-dimensional encoding of a 784-dimensional image. We define the decoder in analogous fashion using three layers of transposed convolutional GPs, again with 384 inducing patches $\mathbf{Z} \in \mathbb{R}^{3 \times 3 \times c_{t-1}}$ shared between $\{32, 32, 32\}$ latent GPs. A final layer consisting of a single convolutional GP (with the same general outline as above) is used to resolve the penultimate feature map $\mathbb{R}^{28 \times 28 \times 32}$ into a reconstruction of the original image $\mathbb{R}^{28 \times 28 \times 1}$. In all cases, we employ residual connections by using bilinear interpolation to define identity mean functions. Following Salimbeni and Deisenroth (2017), we initialized inducing patches \mathbf{Z} using k -means and inducing distributions q to be nearly deterministic.

Model evaluations are performed by using the sparse update (27) together with functions drawn from approximate priors constructed using $\ell = 256$ random Fourier features. We associate each input with a single realization of the model. Running on a single GPU, the entire model was jointly trained in just over 40 minutes using 10^4 steps of gradient descent with a batch size of 128. Figure 8 visualizes the (distribution of) reconstructions for a randomly chosen set of test images.

10. Note that this cost is separately incurred by each input to each layer, see Dutordoir et al. (2020).

8. Conclusion

Throughout this work, we have used Matheron’s update rule (Theorem 1) as the impetus for looking at Gaussian processes in a different light. This simple equivalence,

$$(\mathbf{a} \mid \mathbf{b} = \boldsymbol{\beta}) \stackrel{\text{d}}{=} \mathbf{a} + \boldsymbol{\Sigma}_{\mathbf{a},\mathbf{b}} \boldsymbol{\Sigma}_{\mathbf{b},\mathbf{b}}^{-1} (\boldsymbol{\beta} - \mathbf{b}), \quad (4)$$

allows us to think about GP posteriors in terms of random functions. Doing so not helps to clarify existing ideas, but enables us to envision new ones. As it turns out, many of these ideas are intimately practical.

Throughout this work, we have repeatedly stressed how Matheron’s update rule separates out Gaussian priors from data-drive pathwise updates. We may then leverage these objects’ mathematical properties to construct efficient approximators. As a rule, however, the patterns at play in both cases are fundamentally different: priors typically admit convenient global trends, whereas data often exhibits localized structure. Fully exploiting these properties therefore requires us to take advantage of different representations, for example different basis expansions, for each term. Decomposing GP posteriors into global and local terms makes this particularly easy.

Pathwise and distributional conditioning are complementary viewpoints that give rise to complementary methods. In cases where the quantity of interest is readily obtainable by working with (finite-dimensional) marginal distributions, distributions act as a natural lens for viewing Gaussian process posteriors. On the other hand, when a problem involves arbitrarily many random variables, random functions provide a more direct path to efficient solutions.

All said and done, pathwise conditioning is a powerful tool for both reasoning about and working with GPs. Methods that fit this mold are generally straightforward to use and can easily be tailored to fully exploit the properties of individual tasks. We have done our best to overview, what we feel to be, key ingredients for efficiently sampling from Gaussian process posteriors and look forward to learning more about related ideas alongside you, the reader.

Acknowledgments

J.T.W. was supported the EPSRC Centre for Doctoral Training in High Performance Embedded and Distributed Systems, reference EP/L016796/1. V.B. and P.M. were supported by “Native towns”, a social investment program of PJSC Gazprom Neft and by the Ministry of Science and Higher Education of the Russian Federation, agreements N° 075-15-2019-1619 and N° 075-15-2019-1620. A.T. was supported by the Department of Mathematics at Imperial College London.

References

- J. Bect, D. Ginsbourger, L. Li, V. Picheny, and E. Vazquez. Sequential design of computer experiments for the estimation of a probability of failure. *Statistics and Computing*, 22(3):773–793, 2012. Cited on page 2.

- K. Blomqvist, S. Kaski, and M. Heinonen. Deep convolutional Gaussian processes. In *Joint European Conference on Machine Learning and Knowledge Discovery in Databases*, pages 582–597. Springer, 2019. Cited on page 29.
- V. Borovitskiy, I. Azangulov, A. Terenin, P. Mostowsky, M. P. Deisenroth, and N. Durrande. Matern Gaussian Processes on Graphs. *arXiv:2010.15538*, 2020. Cited on page 12.
- V. Borovitskiy, A. Terenin, P. Mostowsky, and M. P. Deisenroth. Matern Gaussian processes on Riemannian manifolds. In *Advances in Neural Information Processing Systems*, 2020. Cited on page 12.
- D. Calandriello, L. Carratino, A. Lazaric, M. Valko, and L. Rosasco. Gaussian process optimization with adaptive sketching: scalable and no regret. In *Conference on Learning Theory*, pages 533–557, 2019. Cited on page 14.
- P. E. Castro, W. H. Lawton, and E. Sylvestre. Principal modes of variation for processes with continuous sample curves. *Technometrics*, 28(4):329–337, 1986. Cited on page 12.
- G. Chan and A. T. Wood. Algorithm AS 312: An algorithm for simulating stationary Gaussian random fields. *Applied Statistics*:171–181, 1997. Cited on page 11.
- O. Chapelle and L. Li. An empirical evaluation of Thompson sampling. In *Advances in Neural Information Processing Systems*, pages 2249–2257, 2011. Cited on page 25.
- J.-P. Chiles and P. Delfiner. *Geostatistics: Modeling Spatial Uncertainty*. Wiley, 2009. Cited on pages 2, 9.
- J.-P. Chilès and C. Lantuéjoul. Prediction by conditional simulation: models and algorithms. In *Space, Structure and Randomness*, pages 39–68. Springer, 2005. Cited on page 9.
- M. Cuturi. Sinkhorn distances: lightspeed computation of optimal transport. In *Advances in Neural Information Processing Systems*, pages 2292–2300, 2013. Cited on page 26.
- A. Damianou and N. Lawrence. Deep Gaussian processes. In *Artificial Intelligence and Statistics*, pages 207–215, 2013. Cited on pages 15, 29.
- C. de Fouquet. Reminders on the conditioning Kriging. In *Geostatistical Simulations*, pages 131–145. Springer, 1994. Cited on page 9.
- M. P. Deisenroth and C. E. Rasmussen. PILCO: A model-based and data-efficient approach to policy search. In *International Conference on Machine Learning*, 2011. Cited on pages 2, 26.
- C. R. Dietrich and G. N. Newsam. Fast and exact simulation of stationary Gaussian processes through circulant embedding of the covariance matrix. *SIAM Journal of Scientific Computing*, 18:1088–1107, 1997. Cited on page 11.

- A. Doucet. A note on efficient conditional simulation of Gaussian distributions. Technical report, University of British Columbia, 2010. Cited on page 9.
- N. Durrande, V. Adam, L. Bordeaux, S. Eleftheriadis, and J. Hensman. Banded matrix operators for Gaussian Markov models in the automatic differentiation era. In *Artificial Intelligence and Statistics*, pages 2780–2789, 2019. Cited on page 11.
- V. Dutordoir, M. Wilk, A. Artemev, and J. Hensman. Bayesian Image Classification with Deep Convolutional Gaussian Processes. In *Artificial Intelligence and Statistics*, pages 1529–1539. PMLR, 2020. Cited on page 29.
- X. Emery. Conditioning simulations of Gaussian random fields by ordinary Kriging. *Mathematical Geology*, 39(6):607–623, 2007. Cited on page 9.
- L. C. Evans. *Partial Differential Equations*. American Mathematical Society, 2010. Cited on page 13.
- R. FitzHugh. Impulses and physiological states in theoretical models of nerve membrane. *Biophysical Journal*, 1(6):445, 1961. Cited on page 27.
- P. I. Frazier. A tutorial on Bayesian optimization. *arXiv:1807.02811*, 2018. Cited on page 24.
- K. Fukunaga. *Introduction to Statistical Pattern Recognition*. Elsevier, 2013. Cited on page 12.
- J. Gardner, G. Pleiss, K. Q. Weinberger, D. Bindel, and A. G. Wilson. GPyTorch: Blackbox matrix-matrix Gaussian process inference with GPU acceleration. In *Advances in Neural Information Processing Systems*, pages 7576–7586, 2018. Cited on pages 15, 17.
- A. Grigoryan. *Heat Kernel and Analysis on Manifolds*. American Mathematical Society, 2009. Cited on page 13.
- P. Hegde, M. Heinonen, H. Lähdesmäki, and S. Kaski. Deep learning with differential Gaussian process flows. *arXiv:1810.04066*, 2018. Cited on page 29.
- J. Hensman, N. Fusi, and N. D. Lawrence. Gaussian processes for big data. In *Uncertainty in Artificial Intelligence*, pages 282–290, 2013. Cited on page 16.
- J. Hensman, A. Matthews, and Z. Ghahramani. Scalable variational Gaussian process classification. In *Artificial Statistics and Machine Learning*, 2015. Cited on page 15.
- J. M. Hernández-Lobato, J. Requeima, E. O. Pyzer-Knapp, and A. Aspuru-Guzik. Parallel and distributed Thompson sampling for large-scale accelerated exploration of chemical space. In *International Conference on Machine Learning*, pages 1470–1479, 2017. Cited on page 25.
- Y. Hoffman and E. Ribak. Constrained realizations of Gaussian fields: a simple algorithm. *The Astrophysical Journal*, 380:L5–L8, 1991. Cited on page 9.

- A. G. Journel and C. J. Huijbregts. *Mining Geostatistics*. Academic Press, 1978. Cited on pages 2, 9.
- O. Kallenberg. *Foundations of Modern Probability*. Springer, 2006. Cited on page 5.
- S. Kamthe and M. P. Deisenroth. Data-efficient reinforcement learning with probabilistic model predictive control. In *Artificial Intelligence and Statistics*, pages 1701–1710, 2018. Cited on page 26.
- M. Kanagawa, P. Hennig, D. Sejdinovic, and B. K. Sriperumbudur. Gaussian processes and kernel methods: A review on connections and equivalences. *arXiv:1807.02582*, 2018. Cited on page 23.
- K. Kandasamy, A. Krishnamurthy, J. Schneider, and B. Póczos. Parallelised Bayesian optimisation via Thompson Sampling. In *Artificial Intelligence and Statistics*, pages 133–142, 2018. Cited on page 25.
- E. T. Krainski, V. Gómez-Rubio, H. Bakka, A. Lenzi, D. Castro-Camilo, D. Simpson, F. Lindgren, and H. Rue. *Advanced spatial modeling with stochastic partial differential equations using R and INLA*. CRC Press, 2018. Cited on pages 12, 13.
- M. Lázaro-Gredilla and A. Figueiras-Vidal. Inter-domain Gaussian processes for sparse inference using inducing features. In *Advances in Neural Information Processing Systems*, pages 1087–1095, 2009. Cited on page 16.
- Y. LeCun and C. Cortes. MNIST handwritten digit database, 2010. URL: <http://yann.lecun.com/exdb/mnist/>. Cited on page 29.
- M. Lifshits. *Lectures on Gaussian Processes*. Springer, 2012. Cited on page 13.
- F. Lindgren, H. Rue, and J. Lindström. An explicit link between Gaussian fields and Gaussian Markov random fields: the stochastic partial differential equation approach. *Journal of the Royal Statistical Society: Series B (Statistical Methodology)*, 73(4):423–498, 2011. Cited on pages 12, 13.
- J. Loper, D. Blei, J. P. Cunningham, and L. Paninski. General linear-time inference for Gaussian Processes on one dimension. *arXiv:2003.05554*, 2020. Cited on page 11.
- G. J. Lord, C. E. Powell, and T. Shardlow. *An introduction to computational stochastic PDEs*. Cambridge University Press, 2014. Cited on pages 5, 12, 13.
- J. Moćkus. On Bayesian methods for seeking the extremum. In *Optimization techniques IFIP technical conference*, pages 400–404. Springer, 1975. Cited on page 24.
- M. Mutny and A. Krause. Efficient high dimensional Bayesian optimization with additivity and quadrature Fourier features. In *Advances in Neural Information Processing Systems*, pages 9005–9016, 2018. Cited on page 14.

- J. Nagumo, S. Arimoto, and S. Yoshizawa. An active pulse transmission line simulating nerve axon. *Proceedings of the Institute of Radio Engineers*, 50(10):2061–2070, 1962. Cited on page 27.
- H. Nickisch and C. E. Rasmussen. Approximations for binary Gaussian process classification. *Journal of Machine Learning Research*, 9:2035–2078, 2008. Cited on page 15.
- D. S. Oliver. On conditional simulation to inaccurate data. *Mathematical Geology*, 28(6):811–817, 1996. Cited on page 9.
- M. Oppor and C. Archambeau. The variational Gaussian approximation revisited. *Neural computation*, 21(3):786–792, 2009. Cited on page 17.
- A. Parker and C. Fox. Sampling Gaussian distributions in Krylov spaces with conjugate gradients. *SIAM Journal on Scientific Computing*, 34(3):B312–B334, 2012. Cited on page 17.
- G. Pleiss, J. R. Gardner, K. Q. Weinberger, and A. G. Wilson. Constant-time predictive distributions for Gaussian processes. In *International Conference on Machine Learning*, pages 4114–4123, 2018. Cited on pages 11, 17, 18.
- G. Pleiss, M. Jankowiak, D. Eriksson, A. Damle, and J. R. Gardner. Fast matrix square roots with applications to Gaussian processes and Bayesian optimization. *arXiv:2006.11267*, 2020. Cited on page 17.
- J. Quinero-Candela, C. E. Rasmussen, and C. K. I. Williams. Approximation methods for Gaussian process regression. In *Large-scale Kernel Machines*, pages 203–223. MIT Press, 2007. Cited on pages 16, 18.
- A. Rahimi and B. Recht. Random features for large-scale kernel machines. In *Advances in Neural Information Processing Systems*, pages 1177–1184, 2008. Cited on page 11.
- C. E. Rasmussen and J. Quinero-Candela. Healing the relevance vector machine through augmentation. In *International Conference on Machine Learning*, pages 689–696, 2005. Cited on page 18.
- C. E. Rasmussen and C. K. I. Williams. *Gaussian Processes for Machine Learning*. MIT Press, 2006. Cited on pages 1, 10, 14, 15, 17.
- J. L. Rodgers, W. A. Nicewander, and L. Toothaker. Linearly independent, orthogonal, and uncorrelated variables. *The American Statistician*, 38(2):133–134, 1984. Cited on page 5.
- H. Rue and L. Held. *Gaussian Markov random fields: theory and applications*. CRC Press, 2005. Cited on pages 11, 27.
- H. Salimbeni and M. P. Deisenroth. Doubly Stochastic Variational Inference for Deep Gaussian Processes. In *Advances in Neural Information Processing Systems*, 2017. URL: <https://arxiv.org/abs/1705.08933>. Cited on page 29.

- B. Schölkopf and A. J. Smola. *Learning with Kernels: Support Vector Machines, Regularization, Optimization, and Beyond*. MIT Press, 2001. Cited on page 11.
- M. Seeger. Bayesian methods for support vector machines and Gaussian processes. Technical report, 1999. Cited on page 17.
- B. Shahriari, K. Swersky, Z. Wang, R. P. Adams, and N. de Freitas. Taking the human out of the loop: a review of Bayesian optimization. *Proceedings of the IEEE*, 104(1):148–175, 2015. Cited on page 2.
- A. J. Smola and P. L. Bartlett. Sparse greedy Gaussian process regression. In *Advances in Neural Information Processing Systems*, pages 619–625, 2001. Cited on page 18.
- E. Snelson and Z. Ghahramani. Sparse Gaussian processes using pseudo-inputs. In *Advances in Neural Information Processing Systems*, pages 1257–1264, 2006. Cited on page 16.
- J. Snoek, H. Larochelle, and R. P. Adams. Practical Bayesian optimization of machine learning algorithms. In *Advances in Neural Information Processing Systems*, pages 2951–2959, 2012. Cited on page 25.
- A. Solin and M. Kok. Know your boundaries: Constraining Gaussian processes by variational harmonic features. In *Artificial Intelligence and Statistics*, 2019. Cited on pages 12, 27, 28.
- A. Solin and S. Särkkä. Hilbert space methods for reduced-rank Gaussian process regression. *Statistics and Computing*, 30(2):419–446, 2020. Cited on page 12.
- N. Srinivas, A. Krause, S. M. Kakade, and M. Seeger. Gaussian process optimization in the bandit setting: No regret and experimental design. *arXiv:0912.3995*, 2009. Cited on page 24.
- D. J. Sutherland and J. Schneider. On the error of random Fourier features. In *Uncertainty in Artificial Intelligence*, pages 862–871, 2015. Cited on pages 12, 21.
- W. R. Thompson. On the likelihood that one unknown probability exceeds another in view of the evidence of two samples. *Biometrika*, 25(3/4):285–294, 1933. Cited on page 25.
- M. K. Titsias. Variational learning of inducing variables in sparse Gaussian processes. In *Artificial Intelligence and Statistics*, pages 567–574, 2009. Cited on pages 15, 16.
- M. Titsias and N. D. Lawrence. Bayesian Gaussian process latent variable model. In *Artificial Intelligence and Statistics*, pages 844–851, 2010. Cited on page 15.
- M. van der Wilk, V. Dutordoir, S. T. John, A. Artemev, V. Adam, and J. Hensman. A framework for interdomain and multioutput Gaussian processes. *arXiv:2003.01115*, 2020. Cited on page 29.

- M. van der Wilk, C. E. Rasmussen, and J. Hensman. Convolutional Gaussian processes. In *Advances in Neural Information Processing Systems*, pages 2849–2858, 2017. Cited on page 29.
- G. Wahba. *Spline models for observational data*. Society for Industrial and Applied Mathematics, 1990. Cited on page 18.
- K. Wang, G. Pleiss, J. Gardner, S. Tyree, K. Q. Weinberger, and A. G. Wilson. Exact Gaussian processes on a million data points. In *Advances in Neural Information Processing Systems*, pages 14622–14632, 2019. Cited on page 17.
- Z. Wang, C. Gehring, P. Kohli, and S. Jegelka. Batched large-scale Bayesian optimization in high-dimensional spaces. In *Artificial Intelligence and Statistics*, pages 745–754, 2018. Cited on page 14.
- P. Whittle. Stochastic processes in several dimensions. *Bulletin of the International Statistical Institute*, 40(2):974–994, 1963. Cited on page 27.
- A. Wilson and H. Nickisch. Kernel interpolation for scalable structured Gaussian processes. In *International Conference on Machine Learning*, pages 1775–1784, 2015. Cited on pages 11, 18.
- J. T. Wilson, V. Borovitskiy, A. Terenin, P. Mostowski, and M. P. Deisenroth. Efficiently sampling functions from Gaussian process posteriors. In *International Conference on Machine Learning*, pages 7470–7480, 2020. Cited on pages 20, 21, 24, 25.
- H. Zhu, C. K. Williams, R. Rohwer, and M. Morciniec. Gaussian regression and optimal finite dimensional linear models. Technical report, Aston University, 1997. Cited on page 12.